SPECTRAL INVESTIGATIONS OF AURORAE AND TWILIGHT

BY *L. VEGARD* AND *G. KVIFTE*

(Manuscript received February 2, 1945.)

§ 1. Introductory Remarks.

In the present paper we intend to deal with results of investigations which include the following three subjects:

I. Results obtained from auroral spectrograms taken at Oslo during the years 1941—43.

II. Tables giving wave-lengths and possible interpretations of the lines and bands hitherto observed in the auroral luminescence.

III. The origin of the yellow sodium line in twilight and the determination of the upper limit of the atmospheric layer from which the sodium line mainly originates and the height of the screening layer which cuts out the exciting solar radiation.

These three subjects might have been treated in separate papers, but as they are all intimately connected with the physics of the upper atmosphere, we have preferred to unite them into one paper.

CHAPTER I

Results Obtained from Auroral Spectrograms taken at Oslo during the Years 1941—43.

§ 2. Remarks on the Observational Work.

The auroral spectrograms to be dealt with in this paper were taken from the roof of the Physics Building at Blindern, Oslo with two spectrographs of high light power, which will be denoted by (a) and (C).

The spectrograph (a) was built in 1922 and was described in a previous paper.[1]

The camera lens was an Ernemann Kinostigmat (F : 2) with a focal distance of 6 cm. The collimator lens had a focal distance of 20 cm. The instrument had one Rutherford prism.

The spectrograph (C), which was built in 1939—40, was considerably larger than the one (a) mentioned above. It combined a higher light power with a larger dispersion. It had an Astro Camera lens (F : 0.95) with an aperture of 8 cm and focal length 7.5 cm.

The dispersion curve was given in a previous paper (2), where reproductions of some auroral and twilight spectrograms taken with this instrument were reproduced.

The spectrographs were mounted with the slit horizontal and in such a way that they could be turned round a vertical and a horizontal axis. The angle between the collimator axis and the horizontal plane could be measured.

A lens was placed in front of the slit and at a distance from it equal to the focal length of the lens. By means of this lens a picture of the part of the sky aimed at is thrown on the slit, and the light entering the instrument thus comes from a narrow horizontal stripe of the sky passing through the point where the direction of the collimator axis cuts the sky. This arrangement is essential when we want to study spectral changes with the altitude or with the zenith-distance.

---

[1] No. 1 in the list of papers.

§ 3. Plan and purpose of the observations.

The main object of taking spectrograms with such a fairly small dispersion is to study the spectral types obtained from various auroral displays and under varying conditions and to measure variations in the relative intensity distribution of known lines and bands.

As is well known, the intensity distribution within the auroral spectrum varies considerably with the altitude, and although a number of altitude effects have been described in previous papers a further study of these effects will be of interest.

We have therefore tried — as far as possible — to obtain on the same plate at least two auroral spectrograms, one corresponding to the lower, the other to the upper part of auroral rays (R), draperies (D) or arcs (A).

It is, however, not always that an auroral display is suitable for such a procedure, and in those cases we have taken spectrograms by keeping on directing the collimator towards the part of the sky where the aurorae are particularly strong.

As a rule the aurorae have their maximum intensity near the lower limit. These spectrograms corresponding to various forms, may therefore be expected to give an intensity distribution of the type observed for the lower border.

Variations of intensity distribution within the auroral spectrum due to various causes have been dealt with in a number of previous papers, see e. g. Nos. 3, 4, 5, 6, 7, 8 in the list of papers.

In this connection we shall mention some variational effects which are of particular interest in connection with the study and discussion of our auroral spectrograms.

1. The intensity of the negative nitrogen bands relative to that of the green line increases with the altitude. The effect which was detected by Vegard in 1923 (3.4) has had far-reaching consequences for our knowledge of the physical state of the upper atmosphere.
2. The red aurorae of type (A) owe their redness mainly to the enhancement of the red OI-triplet, which follows the variation of sunspot frequency. The effect was found by Vegard in 1926 (5).
3. The intensity of the red OI-triplet relative to that of the green line increases with the altitude. The effect which was detected in 1936 (9.10) is not restricted to red aurorae of type A, but seems to hold good independently of colour, auroral type and sunspot frequency. It will therefore be of interest to continue the observations of this effect to see how far it holds good generally.
4. The bands of the 1st positive group, many of which appear in the red part — are considerably enhanced as we pass downwards. And this effect, which was discovered in 1937 (7), is responsible for the red aurorae of type B for which the red colour is restricted to the bottom part. Height measurements (11) indicate that aurora of this type reach down to very low altitudes of say 65—80 km.
5. When the aurorae appear in a region exposed to sunlight, the red tripled and also to a certain extent bands of the 1st positive group and the negative bands are enhanced relatively to the intensity of the green line. Those effects were described by Vegard in 1937 (compare papers 19 and 6).
6. From the intensity distribution within a rotational band we can find an upper limit of the temperature of that part of the auroral region from which the light analysed is emitted. (1, 12, 13, 14, 15, 16, 17, 18). By comparing bands corresponding to the lower and upper parts of the auroral streamers possible temperature variations with the altitude may be detected and measured. Some work in this direction has already been done (15).

   The spectrograph (C) which combines a fairly good dispersion with great light power might be well adapted for the search for such an effect.
7. The hydrogen lines (H_α, H_β), which as a rule are too weak to be detected in auroral spectro grams, may occasionally appear quite distinctly, indicating that showers of hydrogen penetrate into the higher strata of the atmosphere. Continued investigations of the enhancement of the hydrogen lines are of very great interest in connection with the study of solar and terrestrial relationships. Thus it is of interest to see whether and in which way the occurrance of hydrogen showers is connected with some type of solar activity.

8. The yellow sodium doublet (D_1D_2) which appears with great intensity in the twilight, is also found in the spectra from Aurorae and the night sky. The sodium lines like those of hydrogen show considerable intensity fluctuations which indicate that the appearance of the (D_1D_2) doublet is closely related to solar processes. The study of these fluctuations is, therefore, a matter of great importance.

§ 4. The Auroral Spectrograms.

A selection of the somewhat successful auroral spectrograms obtained at Oslo during the period 1941—43 are reproduced on Plate I. Details regarding each spectrogram are given in the explanation of Plate I at the end of the paper. The spectrograms on Plate I are arranged in groups in such a way that those which have been taken on the same photographic plate are put close to each other and form a group.

On spectrogram No. 1 some of the stronger lines and bands are indicated by the letter a, b, c, d, e, f, g, h, i, and their wave-length and identification are given in Table I. These lines and bands are useful for orientation, as they may easily be recognized on any of the other spectrograms on which they appear.

The capital letters put to the right of each spectrogram on Plate I have the following signification:

L: Spectrogram from Lower border.
U: » » Upper »
V: Spectrogram from the strongest parts of various aurorae. Will usually be of the type (L.).
C: Spectrograms from the region near the convergence point of a "Corona". Will be of the type (U.).
S: Spectrograms from sunlit aurorae.

§ 5. The Wave-length Measurements.

The stronger lines and bands can be identified directly by looking at the spectrograms. Wave-length measurements were therefore only undertaken for spectrograms sufficiently exposed to show a number of weak lines, which we want to identify.

Some of the stronger lines and bands given in Table I have been used as standards of reference.

Table I.

Letter	Wave-length	Identification
a	5577.35	Strong green O I-line
b	6300.30	Strong red O I-line
c	6564.	Hα
d	5202. 5270.	Bands and lines of unknown origin, often called second green line
e	5006.8	Nebular O III-line
f	4861.5	Hβ
g	4709.	Neg. Nitrogen band. N_2^+ (0—2)
h	4278.	Neg. Nitrogen band. » (0—1)
i	3914.	Neg. Nitrogen band. » (0—0)

The results of the wave-length measurements are given in Table II a. With the exception of a faint line or band with the mean wave-length 6231, all the weak lines have been identified as lines known from previous observations. We want to call attention to some interesting facts in connection with the appearance of certain lines.

On the spectrograms from September 1941 the Hβ line is very weak and is only observed on the heavily exposed spectrograms Nos. 1 and 3, and not on the fairly strong spectrogram No. 6. On these spectrograms the yellow sodium line (D_1D_2) (5892) does not appear at all. On the spectrograms from the winter 1942—43 the sodium line is quite strong even in the middle of the night, see e. g. the spectrograms Nos. 22, 29, 30 and 31. On the spectrograms Nos. 27 and 28 the Hβ line is particularly strong. It appears with a photographic density equal to that of the negative band 4709. *Our spectrograms thus illustrate in a striking manner the large fluctuations in the intensity of the hydrogen and sodium lines, indicating relatively large fluctuations in the concentration of these substances within the auroral region.*

It is a matter of interest to notice that the lines 6157 and 5993, which both within the limit of error coincide with OI-lines, appear quite distinctly on some of our spectrograms. The line 5993 also nearly coincides with a band of the 1st positive group of nitrogen; but in that case we should expect a number of other bands of this group to appear. On spectrogram No. 6, however, only these two lines appear in the interval between the green auroral line and the red triplet. On spectrogram No. 22 only these two lines and the yellow sodium line appear in the same spectral interval.

Table II a.

Wave-lenght values from Spectrograms taken at Oslo with Spectrograph C on Agfa I.S.S. plates.

	Not sensitized			Sensitized with NH_3							Interpretation
Spectra Pl. I No.	1	3	6	22	26	27	28	29	30	31	
Date	$^{18}/_{9}$—41	$^{19}/_{9}$—41	$^{19}/_{9}$—41	$^{11}/_{10}$—42	$^{8}/_{12}$—42	$^{11}/_{3}$—43	$^{11}/_{3}$—43	$^{12}/_{3}$—43	$^{12}/_{3}$—43	$^{12}/_{3}$—43	
Exposure	21^{30}—23^{35}	01^{30}—03^{15}	20^{47}—21^{48}	22^{00}—05^{00}	23^{30}—03^{30}	19^{52}—21^{07}	21^{07}—01^{00}	01^{00}—04^{00}	20^{20}—23^{50}	23^{50}—03^{15}	
Aur. Form	Various	Surfaces R	Lower lim. A	Lower lim. A	Lower lim. A	Upper lim. A	Lower lim. A	Upper lim. A	Upper lim. A	Lower lim. A	
Previously measured	λ	λ	λ	λ	λ	λ	λ	λ	λ	λ	
6564	6555	6564	(6553)	6560	6567	6564	6566	-	-	-	Hα, 1. P. G.
6543 6526	6530	6538	6528	-	-	-	-	6538	-	-	1. P. G. 7—4
6469 6441	6442	6449	6444	6462	6452	6471	6471	-	-	-	1. P. G. 8—5
6363.7	6366	6362	6365	6365	6365	6364	6367	6364	6365	6360	OI
6300.3	6300	6300	6300	6300	6300	6300	6300	6300	6300	6300	OI
	6227	6228	-	6234	-	6231	6237	-	-	-	
6175 6138	6145	(6126)	6135	6157	-	-	6156	-	-	-	OI (6158, 6157, 6156)
6108	(6108)	-	-	(6109)	-	-	(6111)	-	-	-	1. P. G. 13—10, 19—17
6058	-	6054	-	-	-	-	6050	-	-	-	OI (6046)
5990.8	5991	5989	5997	5998	5990	-	5993	-	-	-	OI (5995) 1. P. G. 15—12
5966	5969	-	-	-	-	-	-	-	-	-	1. P. G. 8—4
5891	-	-	-	5891	5894	-	5889	5890	5890	5891	NaI (D_1D_2)
5680	-	-	-	-	-	-	5678	-	-	-	NII (5676, 5679)
5577.34	5577	5577	5577	5577	5577	5577	5577	5577	5577	5577	OI
5287 5255	5269	5271	-	-	-	-	-	-	-	-	
5202	5208	5201	-	5204	-	-	5206	-	-	-	
5006.8	5005	5005	-	-	-	-	5004	-	-	-	OIII Neb.
4861.5	4858	4862	-	-	-	4864	4863	-	-	-	Hβ
4780	4782	4772	-	-	-	-	4765	-	-	-	OI (4773)
4709	4709	4710	4709	4709	4709	4708	4709	-	-	-	N. G. 0—2
4652	4649	4650	4651	-	-	-	4652	-	-	-	N. G. 1—3
4596	-	4596	-	-	-	-	4587	-	-	-	N. G. 2—4
4554	-	4559	-	-	-	-	-	-	-	-	N. G. 3—5
4535	-	4530	-	-	-	-	-	-	-	-	ε (3—15) NIII (4535, 4531)
4484	-	4478	-	-	-	-	-	-	-	-	N. G. 5—7
4437	-	4434	-	-	-	-	-	-	-	-	NII (4433)
4415.3	4421	-	-	-	-	-	-	-	-	-	OII (4415, 4417)
4368.3	4369	4370	-	-	-	-	4370	-	-	-	OI (4368.3)
4339.7	4340	4342	-	-	-	-	4340	-	-	-	Hγ ε (1—13)
4319	-	4319	-	-	-	-	4323	-	-	-	OII (4319.7)
4305	4303	-	-	-	-	-	-	-	-	-	OII (4304)
4277.6	4278	4278	4278	4278	4278	4278	4278	4278	4278	-	N. G. 0—1
4236	4236	4236	-	4237	-	-	4235	-	-	-	N. G. 1—2
4200	-	-	-	-	-	-	-	-	-	-	N. G. 2—3
3914	3914	3914	3914	3914	-	-	3914	-	-	-	N. G. 0—0

These facts indicate that the lines 6157 and 5993 appearing on the two spectrograms do not belong to the 1st positive groups, but are to be identified with the OI triplet (6158, 6157, 6156) and the OI-line 5995 respectively.

§ 6. Enhancement of OII-Lines with the Altitude.

The three spectrograms Pl. I No. 16 a, 16 b, and 17 from March 1942 were taken with the new spectrograph C and on "Agfa spektral Blau Ultra rapid plates", which are very sensitive in blue and violet. They were taken for the main purpose of detecting a possible temperature variation with the altitude.

Two of the spectrograms, 16 a and 17, correspond to the lower, and 16 b to the upper limit of auroral arcs and rays.

The question of the temperature will be dealt with later on in § 8. What interests us in this connection is the very important fact that *the spectrogram from the upper limit shows, in the blue part, a number of lines which do not appear on the spectograms 16 a and 17 corresponding to the lower border.* On account of the great interest attached to these spectral changes with the altitude two of the spectrograms, 16 a and 16 b, which were taken on the same plate, are reproduced in a much larger scale on Pl. II. The fact that a number of weak lines in blue are considerably enhanced with increasing altitude was found by one of us already in 1932 (Cf. paper 1, p. 36). In that case, however, the lines were too indistinct and diffuse for accurate measurements and a correct identification.

During recent years we have acquired a good deal of knowledge regarding the wave-length and interpretation of the weak auroral lines, and from the spectrograms No. 2 on Plate II, we can determine the wave-length of a number of the weaker lines with an accuracy which enables us to identify them as the lines which have previously been measured fairly accurately from spectrograms of greater dispersion.

The results of the wave-length measurements are given in Table II b.

Table II b.

Wave-length Values from Spectrograms taken on Agfa Spectral Blau Plates with Spectrograph (C).

Spectrogram Pl. I No. 16 a	Spectrogram Pl. I No. 16 b	From previous Observations	Interpretation
4709	4709	4709	N. G. 0—2
4652	4649	4652,2	N. G. 1—3, OII (4644,2)
4592	4599	4597	N. G. 2—4, OII (4596,2)
4539		4535	ε 3—15 H_2
	4516	4515	NIII (4515)
4422	4416	4415,3	OII (4417, 4415)
4370	4367	4368,3	OI (4368,3) OII (4369,3)
	4350	4349,3	OII (4349,4)
4338	4334	4335	NI (4336,5), OII (4336,9)
	4318	4319	OII (4319,7)
	4294	4295	OII (4294,8)
4277	4277	4277	N. G. 0—1
4236	4236	4236	N. G. 1—2
3914	3914	3914	N. G. 0—0

In spite of the great density with which the negative bands appear on the spectrogram from the lower limit only a few very faint and diffuse lines can be seen. The wave-length values of these lines given in the 1st column of Table II b are very uncertain. On the spectrogram (Pl. I, 16 b or Pl. II, 2) corresponding to the upper limit a considerable number of weak lines were measured fairly accurately, as is seen by comparing the wave-length values for this spectrogram, given in the 2nd column, with those found previously and given in the 3rd column.

From the last column giving the interpretation of the lines and bands we notice that *most of the lines which are so largely enhanced with the altitude are emitted from singly ionised oxygen atoms.*

One line may possibly be referred to NIII. In one case an OII line nearly coincides with a line from OI, and in one case with a NI line.

The enhancement of lines from ionised oxygen with increasing altitude means that the relative concentration of ionised oxygen atoms increases considerably with the altitude, a result which is in very good agreement with Vegard's view of the physical state of the upper strata of the atmosphere.

§ 7. Measurements of the Intensity Distribution.

By means of an intensity scale photographed on the same plate as the auroral spectrograms, the relative intensities of lines and bands could be measured. The photographic density was evaluated by means of a Moll registering microphotometer. The way in which the relative intensities are found from the photometer diagrams for the auroral spectrograms and the spectrograms of the intensity scale, has been fully dealt with in previous papers. We may, for instance, refer to papers Nos. 1 and 6 in the list.

During a brilliant auroral display which lasted the whole night between Sept. 18—19, we took with the new spectrograph (C) five spectrograms which are reproduced on Pl. I, Nos. 1—5. The spectrograms 1 and 3 show a number of weak lines, the wave-lengths of which are given in Table II a.

Thus we find the nebular line 5006.8 emitted from 0^{2+}-ions and the hydrogen line H_β.

It is particularly interesting to notice that *no trace of the yellow sodium line is to be seen in spite of the great photographic density with which the stronger auroral lines and bands appear.*

The strong exposure of spectrogram No. 3 makes it rather unfit for intensity measurements. As the spectrograms Nos. 1 and 3 seem to have essentially the same intensity distribution, we have only measured the relative intensities for spectrogram No. 1 and for the other three Nos. 2, 4, and 5. The results are given in Table III. Nos. 1 and 2 correspond to a region near the lower border, and give essentially the same intensity distribution. Nos. 4 and 5, which are taken from the region near the convergence point of coronal forms, correspond to a much greater altitude than Nos. 1 and 2. The altitude effects (2) and (3) mentioned above are very pronounced, especially in the case of spectrogram No. 5, which is thus seen to correspond to a somewhat greater average altitude than No. 4. For both spectrograms, however, the two altitude effects are very pronounced.

When the intensity of the green line is put at 100, the intensity of the red line 6300 is 52 in the case of spectrograms from the lower border, and 106 and 140 for the corona spectrograms Nos. 4 and 5 respectively. Taking the intensity of the negative nitrogen band system, the intensity in the case of spectrograms 1 and 2 is 20, and for the corona spectrograms 4 and 5 it is 37 and 71 respectively.

Table III.

Relative Line Intensities (I) from Spectrograms taken with Spectrograph C.

Date	18—19 Sept. 1941			
Sort of Plate	Agfa. I. S. S. not sensitised			
Spectrogr. Pl. I No	1	2	4	5
Expos. Interv.	21^{30}—23^{35}	23^{35}—01^{30}	03^{15}—04^{15}	04^{15}—04^{35}
Direction	N	N	N	N
Height	ca. 20°	ca. 45°	Near Z	Near Z
Aur. Form	Various forms	Various forms	Corona	Corona Violet R
λ	I	I	I	I
H_α 1. P. G.	20	16	23	46
6300 OI	53	51	106	140
6140—6130 1. P. G.	3.0	-	1.9	-
5993 1. P. G.	5.1	4.2	5.6	-
5892 : $D_{1,2}$	-	-	-	-
5577 : OI	100	100	100	100
5240	2.4	3.5	4.2	-
5006 : Nebul	2.8	2.5	2.9	-
4863 : H_β	1.0	-	-	-
4708 : N. G.	6.4	4.5	5.6	12.6
4652 : N. G.	4.4	2.5	2.7	7.2
4596 : N. G.	-	-	1.6	(8.4)
4434—4416	1.3	1.3	-	-
4340 : 2. P. G. H_γ	1.2	1.3	-	(8.1)
4278 : N. G.	20	20	37	71
3236 : N. G.	6.1	5.3	13.3	20
4200 : N G.	-	-	4.8	4.7
3914 : N. G.	36	31	52	97

We might also compare the corona spectrograms Nos. 4 and 5 with the spectrograms Nos. 6, 7, and 8, which we have taken with the same spectrograph in the same condition and on the same kind of plates as the spectrograms Nos. 1—5. No. 6 was taken in the evening of Sept. 19, No. 7 on Sept. 21, and No. 8 on Oct. 11. They all correspond to a region near the lower border, and compared with the corona spectrograms Nos, 4 and 5 they show the two altitude effects in a most striking manner.

The four spectrograms Nos. 9—12 were taken on the same plate during the evening of Oct. 22, 1941. No. 11 corresponds to the lower border, No. 9 to sunlit aurora, and Nos. 10 and 12 to the upper part of rays. The negative bands are rather too weak for intensity measurements, but the green and red OI lines are quite strong.

The results of the intensity measurements for the lines in green and red are given in Table IV

Table IV.

Relative Line Intensities (I) from Spectrograms taken with Spectrograph C.

Date	22—23 Oct. 1941				12 March 1943			11—12 April 1943	
Sort of Plate	Agfa I. S. S. not sens.				Agfa I. S. S. sens. with NH_3			Agfa I. S. S. NH_3 sens.	
Spectr. Pl. I No.	9	10	11	12	29	30	31	32	33
Expos. Interv.	18^{27}—18^{53}	18^{53}—20^{55}	20^{55}—22^{05}	22^{05}—24	01^{00}—04^{00}	20^{20}—23^{50}	23^{50}—03^{15}	22^{30}—00^{40}	00^{40}—01^{40}
Direction	W-N-W	N	N—NE	NNE	N	N	N	N	N
Height	6°—10°	40°—60°	13°	32°	15.5°	15.5°	10°	6.5°	19°
Aur. Form	Sunlit A	Top of R	Lower lim. A & Dr	Top of R	Upper lim. of A	Upper lim. of A	Lower lim. of A	Lower lim. of A	Top of A
	I	I	I	I	I	I	I	I	I
Hα 1. P. G.	19	12	7.2	7.4	-	-	-	13.5	(6.5)
6300 OI	88	63	11.1	73	130	120	(107)	23	118
6140—6130 1. P. G. .	-	-	-	-	-	-	-	1.2	-
5993 1. P. G. OI	-	-	-	-	-	-	-	2.2	-
5892 $D_{1,2}$ Na.......	-	-	-	-	4.8	5.3	12.7	-	-
5577 OI	100	100	100	100	100	100	100	100	100

Comparing the spectrograms Nos. 9 and 11, we notice that *the sunlight effect of the red OI line is very pronounced.* Relative to the green line the intensity of the red line is about 8 times as great in the sunlit atmosphere as under ordinary night conditions represented by spectrogram No. 11. Comparing No. 11 with No. 10 and 12, the intensity of the red line (6300) is seen to increase very much with increasing altitude. A faint line which seems to coincide with Hα also appears with a somewhat varying relative intensity.

Comparing spectrogram No. 13 (Oct. 26, 1941) corresponding to the lower border with spectrogram No. 12 from the upper limit, we see directly from the spectrograms that the intensity of the red triplet and that of the negative nitrogen bands increases with the altitude.

The same two altitude effects are also seen in a most striking way from the spectrograms 14 and 15 of March 3, 1942. The green line is seen to have the greatest density on No. 15 for the lower border while the red triplet and the negative bands have the greatest density on No. 14 from the region near the upper limit. The two spectrograms 16 and 17 taken on Agfa spectral Blau Ultra Rapid plates will be dealt with later on. The four spectrograms Nos. 18—21 were taken on the same plate during the night of Sept. 11—12, 1942, and ought to be strictly comparable. The negative bands are hardly visible. The results of the intensity measurements within the region of long waves are given in Table V. The enhancement of the red line 6300 with increasing altitude is seen to be very pronounced. We ought now to remember that the rest of the spectrograms on Plate I are taken on Agfa I. S. S. plates, sensitized with ammonia, while previously the I. S. S. plates were not sensitized. After the treatment with NH_3 the plates become relatively more sensitive in the long wave part of the spectrum.

In the night from Dec. 8—9 an auroral arc appeared on the northern sky. We took two spectrograms with each of the two spectrographs, one from the lower and one from the upper part. Nos. 23 and 24 were taken with spectrograph (a), Nos. 25 and 26 with spectrograph (C).

On No. 26 the green and red OI lines were too dense for intensity measurements. On this spectrogram the line 5993, the yellow sodium line, Hβ, and the nebulium line 5007 appear, but they are rather weak. On Nos. 23 and 24 the green and red OI lines have a density suitable for intensity measurements. The results which are given in Table V show a considerable enhancement

Table V.

Relative Intensities (I) from Spectrograms taken with Spectrograph a.

Date	11—12 Sept. 1942				8—9 Dec. 1942	
Sort of Plate	Agfa I. S. S. not sensitized				Agfa I. S. S. sens. NH_3	
Spectr. Pl. I No	18	19	20	21	23	24
Exposure	20^{55}—21^{45}	21^{45}—00^{25}	00^{25}—01^{40}	01^{40}—03^{15}	21^{15}—23^{30}	23^{30}—03^{30}
Direction	N	N	N	N	N	N
Height	15°	24°	28°	10°	27°	6—7°
Auroral Form	Lower part of A	Upper lim. A	Top of R	Bottom of R	Upper lim. A	Lower lim. A
λ	I	I	I	I	I	I
1. P. G., Hα	12	-	-	9.1	(73)	41
6300 OI	14	55	52	11.3	113	50
6140 1. P. G. 6130	-	-	-	1.9	-	-
5993 1. P. G.	-	-	6.0	4.6	-	-
5577 OI	100	100	100	100	100	100

of the red triplet on the spectrogram corresponding to the upper limit of the arc.

The spectrograms Nos. 27, 28, and 29 were taken from an arc appearing on the northern sky during the night of March 11—12, 1943, Nos. 27 and 29 corresponding to the upper border, and No. 28 to the lower part of the arc. As the stronger lines and bands of the latter are too dense for intensity measurements, the three spectrograms from this night cannot be used for the study of the altitude effect of the red triplet and of the negative bands. In other respects, however, the spectrograms — and especially No. 28 — show a considerable number of weak lines whose wavelength values were measured and given in Table II. We notice that the lines Hα and Hβ are unusually strong. Both on No. 27 for the upper limit and on No. 28 for the bottom part the density of Hβ is quite as great as that of the band 4709. The yellow sodium line appears very distinctly on these spectrograms Nos. 28 and 29, showing *that this line is found in the auroral luminescence and that the emission may take place in the middle of the night and in higher parts of the auroral region.*

On the spectrograms Nos. 30 and 31, taken in the evening of March 12, the sodium line also appears with considerable intensity in the auroral luminescence, and it is quite as strong from the upper as from the lower part of the arc.

One month later two spectrograms Nos. 32 and 33, corresponding to the lower and upper limit respectively, were taken during the night of April 11—12. Although No. 32 is quite strongly exposed, so that e. g. the weak line 5993 appears quite distinctly, no trace of the yellow sodium line is any longer to be observed. *Thus from March 12 to April 11 the sodium concentration within the auroral region must have diminished very considerably.*

The results of intensity measurements given in Table IV show that the red OI-triplet is considerably enhanced with increasing altitude.

The last three spectrograms on Plate I were taken with the glass spectrograph (a) during the night of Oct. 7—8, 1943. In the region of long waves the instrument was somewhat out of focus, and although the green line and the red triplet — at any rate on the spectrograms Nos. 34 and 35 — are too over-exposed for accurate intensity measurements, the presence of the altitude effect of the negative bands can be distinctly observed from the spectrograms.

Thus on spectrograms Nos. 34 and 35 the green line has about the same density, while the negative bands appear considerably stronger on No. 34 corresponding to the upper limit. On the spectrograms 35 and 36 the negative bands have about the same density, while the green line has a much smaller density on No. 36, corresponding to the upper limit. Here again the sodium line appears, and it is especially quite distinct on the last spectrogram (36), which corresponds to the upper limit.

Since the previous spectrograms (32 and 33) were taken in April, the sodium concentration has again increased. Such fairly rapid fluctuations of the intensity of the yellow sodium line have also been observed previously, both in the Twilight (17), in the auroral luminescence (15, 16, 20), and in the light of the night sky (20).

These fluctuations will be more fully treated in Chapter III, dealing with the appearance of the yellow sodium line in twilight.

§ 8. Does the Temperature of the upper Atmosphere increase with the Altitude?

The method introduced by Vegard in 1923 for the study of possible changes in the spectral composition of the auroral luminescence with increasing altitude, has now been used with great success for years (7, 8, 16, 17), and the results obtained give convincing evidence of its validity.

We have just seen that those of our spectrograms with the proper exposure which have been taken in accordance with this method have in no case failed to bring out the altitude effects. We can therefore safely rely on this method, when we are investigating whether the intensity distribution within a rotational band, in other words the temperature of the ionosphere, changes with the altitude.

During the autumn of 1938 one of us — using a big quartz spectrograph — obtained three spectrograms, which gave the negative band 3914 with a considerable dispersion (34,7 Å/mm) and with a density suitable for intensity measurements. Two of these were taken from the lower border, but one was obtained by directing the collimator systematically towards the upper limit. The results which were given in a previous paper (8) did not indicate any increase of temperature with increasing altitude.

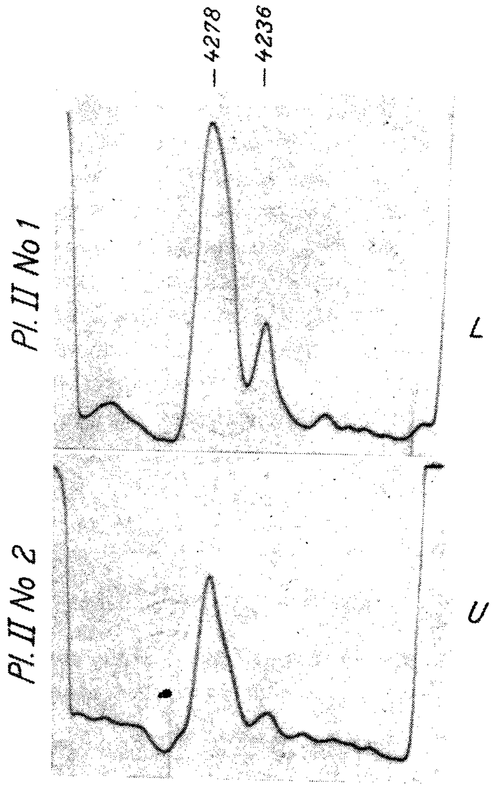

Fig. 1.

Three spectrograms were taken at Oslo with the new spectrograph (C) and on plates (Agfa spectral blau ultra rapid) which are particularly sensitive in the violet. The first spectrogram (Pl. I, No. 16 a and Pl. II. No. 1) was taken on March 5 from the lower part of auroral arcs. The second (Pl. I, No. 16 b and Pl. II, No. 2) was taken during the same night from the top of arcs and rays. A third spectrogram was taken on March 19 from the lower part of arcs.

The dispersion is to small to effect separation of the R- and P-branches, and our usual procedure by determination of the temperature from the intensity distribution within the R-branch cannot be applied. We know, however, that the extention (number of rotational components) of the R-branch increases with temperature.

What chiefly interests us is to know whether any very large increase of temperature with the altitude takes place.

By comparing the extention of the R-branch of the band 4278 on the spectrogram No. 16 b corresponding to the upper limit with the two spectrograms (Nos. 16 a and 17) corresponding to the lower limit, we should be able to detect a great change of temperature if it existed. But no such change of the extension of the R-branch can be observed. In the case of band 4278 the extention of the R-branch can be very accurately estimated from the distance between the limit of the R-branch to band 4236. Photometer curves of bands 4278 and 4236 corresponding to the spectrograms 16 a and 16 b are shown in Fig. 1. Neither the spectrograms nor the photometer curves indicate any widening of the R-branch with increase of altitude. Thus our result is in agreement with that found by one of us from spectrograms taken in 1938 with the large quartz spectrograph.

The question as to whether the temperature increases with the altitude is — from a geophysical point of view — intimately related to the question concerning the temperature derived from aurorae exposed to sunlight.

Spectrograms from sunlit aurorae suitable for temperature measurements have been obtained at Tromsø with spectrographs which have a sufficient dispersion to give a fairly accurately temperature determination. These measurements led to the result (17, 18) that at sunset — when the ionosphere is still exposed to the sun's radiation — the temperature within the auroral region is not essentially higher than in the middle of the night.

Chapter II.

The observed Auroral Lines and Bands and their possible Interpretation.

§ 9. A complete Record of the Auroral Bands and Lines as yet observed and measured.

As the work on the spectral analysis of the Auroral luminescence proceeds, new lines and bands are detected, previously observed lines have been more accurately measured, and the new facts thus accumulated afford new possibilities of finding the correct physical interpretation of the bands and lines. For all those who are interested in this field of research it is, therefore, very useful that every now and then there should be published wave-length tables which are brought up to date and which as far as possible are accompanied by an interpretation of each band and line. A number of such wave-length tables have already been published. Since the last table was published in 1941 (17) a number of new weak lines have been detected and measured, and for some of the lines previously known the accuracy of the wave-length values has been improved (18).

The observational results recently accumulated have also an important bearing on the view we may adopt regarding the interpretation.[1] The bands and lines hitherto observed and measured are collected in Table VI. The first column contains the wave-lengths (λ) and the second the intensities (I) of some of the stronger lines relative to that of the green one, the intensity of which is put equal to 100. As mentioned in Chapter I the intensity distribution is subject to great variations, and the intensities given in Table VI merely represent a kind of typical or average intensity distribution. In the case of certain lines of very great variability we have indicated the interval within which the intensity of the lines has been found to vary.

The bands and lines for which the intensies are not given are all weak. The total number of auroral bands and lines given in Table VI amounts to 173, as against 148 tabulated in the paper of 1941 (17). Most of the lines detected from the spectrograms published in 1944 (18) were referred to neutral or ionised atoms of oxygen.

§ 10 On the Interpretation of Bands and Lines appearing in the Auroral Spectrum.

In the last column of Table VI, giving the interpretation of bands and lines, the following abbreviations have been used:

1. P. G. (n′—n″) means the head of a band belonging to the 1st positive group of nitrogen and corresponding to a transition from a vibrational level with quant number (n′) to one with quant number (n″).

2. P. G. (n′—n″) indicates in a similar way the head of a band belonging to the 2nd positive group of nitrogen.

---

[1] In addition to paper (18) compare also the results given in Chapter I of this paper.

Table VI.

λ	I	Interpretation	λ	I	Interpretation
8132		1. P. G. 5—4, 6—5	5289	6	Band with sharp edge (or line) at 5258
8035			5258		
7906	(47)	1. P. G. 7—6	5230.6		These sharp lines approximately coincide with the lines 5229.4 and 5202.9 of solid N_2 mixed with Neon
7867			5302.9		
7734		1. P. G. 8—7, (2—0)			
7594		1. P. G. 9—8, (3—1)			
7479		1. P. G. (10—9), 4—3; (OI 7477)	5131		OI. 5130.5
7368		1. P. G. (11—10), 5—3	5080		H_2. 5080.5
7264		1. P. G. 6—4; (OI. 7254)	5049		He. 5047.8; NII. 5045.1
7068		1. P. G. 8—6	5029		H_2. 5030.4
6861		1. P. G. 3—0, 10—8	5006.7		OIII. $(^1D_2-{}^3P_2)$ 5006.9 Nebul.
6784		1. P. G. 4—1, 11—9	4987		NII. 4987.3
6768			4975		H_2. 4973.3
6753			4961		OIII. $(^1D_2-{}^3P_1)$ 4959 Nebul.
6696		1. P. G. 5—2, 12—10	4942		OII. 4943, 4941
6682			4935		NI. 4935.
6669			4927		OII. 4925, H_2. 4929
6619		1. P. G. $\begin{Bmatrix}6-3\\13-11\end{Bmatrix}$; NII. 6611; NII. 6584	4916		NI. 4915
6605			4902		OII. 4906.9
6592			4891		OII. 4890 9
6562		Hα. 6562.8	4873		OII. 4871.6
6543		1. P. G. $\begin{Bmatrix}7-4\\14-12\end{Bmatrix}$	4861 5		Hβ. 4861.3; OII. 4861.0
6526			4856		OII. 4856.5
6512			4835		H_2. 4838
6469		NIII. 6466.9	4812		NII. 4810.3
6454		1. P. G. 8—5 OI. 6454.6	4790		NII. 4793.7, 4788.1
6441		OI. 6439.1	4780		ε. 5—17; NII 4779.7, 4781.2, 4774.2
6398		1. P. G. 9—6			
6364	3—200	OI. $(^3P_1-{}^1D_2)$	4746		OII. 4751.3, 4741.7
6300.3	10—600	OI. $(^3P_2-{}^1D_2)$	4709	7.8	N. G. 0—2.
(6229)		?	4652	4.6	N. G. 1—3; OII. 4650.9
6185		1. P. G. 12—9	4633		NIII. 4634; NII. 4631
6176		1. P. G. 18—16	4620		NII. 4621
6154		OI, 6158, 6157, 6156	4597	3.4	N. G. 2—4; OII. 4596.2
6139			4572,3		H_2. 4572.7
6129		1. P. G. 5—1	4565	2.0	NII. 4565
6109		1. P. G. 13—10, 19—17	4554.8		N. G. 3—5; H_2. 4554.2
6068		1. P. G. 6—2; ε. 3—18	4535	1.6	ε. 3—15; H_2 4534.6
6056		OI. 6046	4515		NIII. 4514.9
6010		1. P. G. 7—3	4509	1.0	NIII. 4510.9; NII. 4507.6
6001		NI. 6000	4487.5	1.6	N. G. 5—7; NI. 4488.2
5993	15	1. P. G. 15—12; OI. 5995	4468		OII (4469.4, 4467.8, 4465.4)
5977			4452		OII. 4452.4
5967		1. P. G. 8—4; NII. 5962	4434	1.6	NII. 4432.7
5948		H_2 5947.9; OI. 5951	4427.4	3.0	ε. 2—14
5892		NaI. D_1, D_2, 5890.0, 5895.9	4415.2	2.5	OII (4416.97, 4414.89)
5867	13	1. P. G. 17—14	4403		N (4401). Spark line
5835		1. P. G. $\begin{Bmatrix}18-15\\10-6\end{Bmatrix}$; H_2. 5836	4384		OII. 4380; NIII. 4379
			4377	1.6	OII. 4378.4
5772		NII. 5767	4368.3	2 4	OI. 4368.3; OII. 4369.3
5751		NII $(^1S_0-{}^1D_2)$ 5754 8	4362	1.2	OIII $(^1D_2-{}^1S_0)$ 4363.3 Nebul.
		OI 5750.4; ε. 1—16	4349.2		OII. 4349.4
5743		NII. 5747	4346.5	3.0	2. P. G. 0—4; OII. 4346, 4347
5677		NII. (5676.0, 5679.5)	4340		Hγ. 4340.5 ε (1—13)
5620		1. P. G. 15—11, NI. 5617	4335		NI. 4336.5, OII. 4336.9
5577.345	100	OI $(^1D_2-{}^1S_0)$	4319.5	1.6	OII. 4319.7
5472		1. P. G. 9—4	4305		OII. 4303.8; NI 4305.5
5456		NII. 5454.3	4295		OII. 4294.8
5415		Band with structure	4278	24.4	N. G. 0—1
5403			4236	5.9	N. G. 1—2
5394			4226.3	4.0	NII. 4227.8
5371			4223		NI. 4223
5351			4218	3.0	ε. 0—12, 4218
5332			4200	2.0	N. G. 2—3; NIII 4200
5311			4185.9		OII. 4185.5

Table VI (cont.).

λ	I	Interpretation	λ	I	Interpretation
4176	1.4	ε. 3—14; H_2. 4177.1; NII. 4176	3771.6	1.0	ε. 2—12; NIII. 3771; OIII. 3774
4172		H_2. 4171.3; OII. 4169.2	3755.2	4.2	2. P. G. 1—3; OIII. (3755)
4164		OII. 4169	3728.4	1.0	OII. 3727.8, 3727.3
4141	1.4	2. P. G. 3—7	3711.3	2.4	2. P. G. 2—4; OIII (3715)
4120.4	1.6	OII (4120.3, 4120.6, 4121.5)	3686	1.6	ε. 1—11
4112		OII. 4112.0; NI. 4114.0	3671		2. P. G. 3—5
4092.8	1.6	OII. 4092.9; 2. P. G. 4—8	3603	1.0	ε. 0—10
4076		OII. 4075.9; ε. 2—13	3583	1.6	N. G. 1—0
4059.1	3.4	2. P. G. 0—3	3578	9.8	2. P. G. 0—1
4049		OII. 4048.2	3563.5	1.6	N. G. 2—1
4042		NII (4043.5, 4041.3)	3536.3	4.9	2. P. G. 1—2
4027.5		NII (4026.0)	3503.5	2.2	2. P. G. 2—3
4013			3484	1.0	2. P. G. 7—8; NIV 3483.1
3997.5	3.7	2. P. G. 1—4; NII. 3995.0	3467.5	3.0	2. P. G. 3—4; NI. 3466.5; OII. 3470.4
3982.6	1.0	OII. 3982.7			
3974		OII. 3973.3	3429.0	2.0	ε. 1—10; OIII. 3429
3962.5		OIII. 3961.6	3371.3	9.0	2. P. G. 0—0; NIII (3374, 3367)
3957		NII. 3956; OII. 3954, OI	3339.3	1.2	2. P. G. 1—1; OIII 3340.7
3943	2.2	2. P. G. 2—5	3285.3	1.8	2. P. G. 3—3; OIII. 3385
3915	47.4	N. G. 0—0	3202.7	2.2	ε. (1—9, 7—13)
3884.3	2.2	N. G. 1—1; OII 3883	3192.4		ε. 4—11
3873.8	1.0	OII. (3872.5, 3875.8)	3168.7		2. P. G. 9—7
3857.5		OII. 3857.2; NII. 3855	3159.3	5.8	2. P. G. 1—0
3821.8		OII. 3821.7; NI. 3822.1	3125.7	3.6	2. P. G. 2—1
3805.3	4.9	2. P. G. 0—2; OII 3803	3114.0		2. P. G. 3—2

ε (n′—n″) is the head of a band belonging to the ε-system which was first detected and analised by Vegard, and which is produced by transitions from the electronic A-level to the ground state of the neutral nitrogen molecule. The ε-system is also called the Vegard-Kaplan bands.

N. G. (*n′*—*n″*) means the head of a band belonging to the negative group of nitrogen which is emitted from singly ionized nitrogen molecules.

OI, *OII*, *OIII* are the symbols generally used in spectroscopic work and indicate lines emitted from oxygen atoms that have lost 0, 1, and 2 electrons respectively.

NI, *NII*, *NIII* represent in a similar way lines emitted from atomic nitrogen in a neutral and ionized state.

In the case of the stronger bands and lines the interpretation can be regarded as definitely settled. In the case of some of the weaker lines, however, the error attached to the wave-length may amount to several Å units, and in those cases the interpretation given only means that the line of known origin within the limit of error coincides with the auroral line considered. As appears from Table VI, it often happens that several lines fulfil this condition. But even if there is some uncertainty attached to the interpretation of some of the lines, it is still of interest to call attention to the possible interpretations, which — when the nature of the luminescence is taken into account — may seem to be the most probable.

In what follows we shall make some remarks regarding the correctness of the interpretations given in Table VI.

The following bands and lines are correctly interpreted:

1) The bands referred to the negative group of nitrogen.
2) The bands referred to the 2nd positive group of nitrogen.
3) Most of the bands referred to the 1st positive group of nitrogen.
4) Most of the bands referred to the ε-system of nitrogen.

   The bands of the two latter groups are usually weak and diffuse and in some cases there may be an overlapping between one of these bands and other lines which may be present.
5) The strong green line $OI(^1D_2—^1S_0)$ and the red triplet $OI(^3P_{2,1,0}—^1D_2)$.
6) Lines of the Balmer series of hydrogen occasionally appear.

7) The yellow sodium line sometimes appears with considerable intensity in the auroral luminescence.
8) A considerable number of lines have been referred to neutral oxygen atoms or to the atomic ions OII and OIII. The wave-lengths of some of these have been measured with such accuracy that the error only amounts to a small fraction of an Å-unit, and the coincidence with known lines from atomic oxygen is so close as to leave no doubt as to the correctness of the identifiation. We may, for instance, mention the following lines, the identification of which we regard as settled:

   Line 4368.3 is identical with the strong OI line 4368.3.

   Line 4415.2 is identical with the strong doublet OII (4416.97, 4414.89).

   Lines 4319.5, 4185.9, 3982.6, 3728.4 are no doubt to be identified with the OII lines (4319.7, 4185.9, 3982.7, and 3727.8).

   Line 5006.7, which appears quite isolated, is identical with the nebular line 5006.9 forming the strongest component of the doublet OIII (${}^1D_2$—${}^3P_{2,1}$) and the weaker component 4959 is identical with a faint line 4961 observed on our spectrogram (18) in the auroral luminescence.

   Line 4362 is to be identified with the nebulium line 4363 emitted from the metastable states OIII (${}^1D_2$—${}^1S_0$),

As soon as it had been proved that the strong green and red auroral lines were to be referred to transitions between the metastable ground states of the normal oxygen atom, it became a matter of importance to look for the corresponding nitrogen lines. The question of the possible appearance of these and other atomic nitrogen lines has been discussed in a paper published by Vegard and Tønsberg (17).

From Edlén's determinations of the metastable ground states of NI the following wave-lengths values are found (21):

$$\left.\begin{array}{l}5200.1\\5197.8\end{array}\right\}\ ({}^4S^{3/2}\text{—}{}^2D^{5/2,\ 3/2})$$

$$3466.5\quad ({}^4S^{3/2}\text{—}{}^2P^{1/2,\ 3/2}).$$

The doublet in green, however, cannot be identified with any of the known auroral lines and it is probably too weak to be observed.

The line in ultra violet nearly coincides with a fairly strong auroral line 3467.5. As seen from Table VI, however, this line also nearly coincides with a band of the 2nd positive group and an OII line 3470.4. Although it cannot be considered as proved that line NI (${}^4S$—${}^3P$) appears in the auroral spectrum, it must still be regarded as a very probable interpretation, which has recently been strengthened by the fact that a number of other auroral lines may possibly be referred to neutral or ionized nitrogen atoms.

At the present time, however, we cannot regard the appearance of atomic nitrogen lines as being settled with the same degree of certainty as the appearance of lines from neutral and ionized oxygen atoms.

The dissociation energy of the N_2-molecule being higher than that of the O_2-molecule, we may expect the lines from atomic nitrogen to be weaker than those from atomic oxygen.

A few lines have been referred to the band spectrum of hydrogen (H_2), but these coincidences may perhaps be accidental. In the case of a few auroral lines, we have not ventured to suggest any definite interpretation.

The number of bands and lines which may appear in the auroral spectrum is not to be regarded as exhausted by those given in Table VI. We know from various speatrograms (17, 18) that a number of weak lines appear — e. g. in the region between yellow and violet — which are situated so close together, that they form more or less continuous bands, and only some of the stronger and best separated lines have been measured. A number of weak lines may also be masked by the strong and broad nitrogen bands which always appear.

The number of auroral lines which may be referred to atoms of oxygen or nitrogen in the neutral or ionized state is seen from Table VI to be very considerable, and although in some cases the identification is ambiguous and not conclusive, the number of close coincidences is too large to be merely a matter of chance.

In tables VII and VIII we have collected the atomic O- and N-lines which within the limit of estimated error coincide with observed auroral lines, and we have also added the O- and N-lines which would be masked by the bands from molecular nitrogen or which are situated in an interval which is very crowded with auroral lines and bands.

Table VII. *Atomic Oxygen.*

$\alpha = 2\,s.\ 2\,p.\quad \beta = 2\,s^2.\ 2\,p.\quad \gamma = 2\,s^2.\ 2\,p^2.\quad \delta = 2\,s^2.\ 2\,p^3.\quad \varepsilon = 2\,s^2.\ 2\,p^4.$

OI	
λ	Classification
7476.5	$\delta\ (^2P)\ (3\,s\ ^3P_{012}-3\,p\ ^3D_{123})$
7254.0	$\delta\ (^4S)\ (3\,p\ ^3P_{0\cdot1\cdot2}-5\,s\ ^3S_1)$
6454.6	$\delta\ (^4S)\ (3\,p\ ^5P_2-5\,s\ ^5S^0_2)$
6439.1	
6391	
6375	
6374	$\delta\ (^2D)\ (3\,p\ ^1F_3-4\,d\ ^1G_4)$
6367	$\delta\ (^2D)\ (3\,p\ ^1F_3-4\,d\ ^3G_4)$
6363.7	$\varepsilon\ (^3P_1-{}^1D_2)$
6300 3	$\varepsilon\ (^3P_2-{}^1D_2)$
6158.2	$\delta\ (^4S)\ (3\,p\ ^5P_{3\cdot2\cdot1}-4\,d\,^5D_{0\cdot1\cdot2\cdot3\cdot4})$
6156.8	
6156	
5995.4	$\delta\ (^2D)\ (3\,p\ ^3D_{3\cdot2}-4\,d\ ^3P_2)$
5958.5	$\delta\ (^4S)\ (3\,p\ ^3P_2-5\,d\ ^3D)$
5951	
5750.4	$\delta\ [(^4S)\ 6\,p\ ^3P-(^2D)\ 3\,d\ ^3P_2]$
5577.34	$\varepsilon\ (^1D_2-{}^1S_0)$
5436.8	$\delta\ (^4S)\ (3\,p\ ^5P_{3\cdot2\cdot1}-6\,s\ ^5S_2)$
5435.8	
5435.2	
5330.7	$\delta\ (^4S)\ (3\,p\ ^5P_{3\cdot2\cdot1}-5\,d\ ^5D)$
5329.6	
5329.0	
5130.5	$\delta\ (^4S)\ (3\,p\ ^3P-8\,d\ ^3D)$
4368.3	$\delta\ (^4S)\ (3\,s\ ^3S_1-4\,p\ ^3P_{012})$
3954.6	$\delta\ [(^4S)\ 3\,p\ ^3P_{1\cdot2}-(^2P)\ 3\,s\ ^3P_2]$
3825.1	$\delta\ [(^2D)\ 3\,s\ ^3D_{1\cdot2}-(^2P)\ 3\,p\ ^3D_{1\cdot2\cdot3}]$
3823.5	$\delta\ [(^2D)\ 3\,s\ ^3D_3-(^2P)\ 3\,p\ ^3D_3]$
3692	$\delta\ (^4S)\ (3\,s\ ^3S_1-5\,p\ ^3P)$

OII	
λ	Classification
7321	$\delta\ (^2D^0_5-{}^2P^0_3)$
7335	$\delta\ (^2D^0_3-{}^2P^0_{1,3})$
4943.1	$\gamma\ (^3P)\ (3\,p\ ^2P^0_3-3\,d\ ^2D_5)$
4941.1	$\gamma\ (^3P)\ (3\,p\ ^2P^0_1-3\,d\ ^2D_5)$
4924.5	$\gamma\ (^3P)\ (3\,p\ ^4S^0_3-3\,d\ ^4P_{5\cdot3\cdot1}$
4906.9	
4890 9	
4871.6	$\gamma\ (^1D)\ (3\,p\ ^2P^0_3-3\,d\ ^2D_5)$
4861.0	$\gamma\ (^1D)\ (3\,p\ ^2P_1-3\,d\ ^2D_3)$
4865.0	$\gamma\ (^3P)\ (3\,p\ ^4S^0_3-3\,d\ ^4D_{1\cdot3})$
4856.8	
4856.5	$\gamma\ (^3P)\ (3\,p\ ^4S^0_3-3\,d\ ^2F_5)$
4845.0	$\gamma\ (^3P)\ (3\,p\ ^4S^0_3-3\,d\ ^4D_5)$
4751.3	$\gamma\ (^3P)\ (3\,p\ ^3D^0_5-3\,d\ ^4D_{4\cdot5})$
4741.7	
4710.0	$\gamma\ (^3P)\ (3\,p\ ^2D^0_3-3\,d\ ^2F_5)$
4705	$\gamma\ (^3P)\ (3\,p\ ^2D^0_5-3\,d\ ^2F_7)$
4703	$\gamma\ (^1D)\ (3\,p\ ^2D^0_3-3\,d\ ^2F_5)$
4699.2	$\gamma\ (^3P)\ (3\,p\ ^2D^0_3-3\,d\ ^4D_5)$ $\gamma\ (^1D)\ (3\,p\ ^2D^0_5-3\,d\ ^2F_7)$
4650.9	$\gamma\ (^3P)\ (3\,s\ ^4P_1-3\,p\ ^4D^0_1)$
4596.2	$\gamma\ (^1D)\ (3\,s\ ^2D-3\,p\ ^2F^0)$
4591.0	
4469.4	
4467.8	
4465.4	
4452.4	$\gamma\ (^3P)\ (3\,s\ ^2P_3-3\,p\ ^2D^0_3)$
4417.0	$\gamma\ (^3P)\ (3\,s\ ^2P_1-3\,p\ ^2D^0_3)$
4414.9	$\gamma\ (^3P)\ (3\,s\ ^2P_3-3\,p\ ^2D^0_5)$
4396.0	$\gamma\ (^3P)\ (3\,p\ ^2D^0_5-3\,d\ ^2D_5)$
4379.6	
4378.4	$\gamma\ (^1D)\ (3\,d\ ^2D_{3\cdot5}-4\,f\ ^2F^0_{5,7})$
4369.3	$\gamma\ (^3P)\ (3\,p\ ^2D^0_3-3\,d\ ^2D_3)$
4349.2	
4347.5	$\gamma\ (^1D)\ (3\,s\ ^2D_3-3\,p\ ^2D_3)$
4345.6	$\gamma\ (^3P)\ (3\,s\ ^4P_3-3\,p\ ^4P^0_1)$
4344.4	$\gamma\ (^1D)\ (3\,d\ ^2P_{3\cdot5}-4\,f\ ^2D^0_{3\cdot5})$
4343.3	$\gamma\ (^3P)\ (3\,d\ ^4D_5-4\,f\ ^4D^0_5)$
4336.9	$\gamma\ (^3P)\ (3\,s\ ^4P_3-3\,p\ ^4P^0_3)$
4334.3	$\gamma\ (^3P)\ (3\,d\ ^2F_5-4\,f\ ^4D^0_5)$
4332.8	$\gamma\ (^1D)\ (3\,d\ ^2G_{7\ 9}-4\,f\ ^2G^0_{7\cdot9})$
4319.7	$\gamma\ (^1D)\ (3\,p\ ^2P^0_1-3\,d\ ^2S_1)$
4303.8	$\gamma\ (^3P)\ (3\,d\ ^4P_5-4\,f\ ^4D^0_7)$
4294.8	$\gamma\ (^3P)\ (3\,d\ ^4P_3-4\,f\ ^4D^0_5)$
4275.5	$\gamma\ (^3P)\ (3\,d\ ^4D_7-4\,f\ ^4F^0_9)$
4189.8	$\gamma\ (^1D)\ (3\,p\ ^2F^0-3\,d\ ^2G)$
4185.5	
4169.2	
4121.5	
4120.6	$\gamma\ (^3P)\ (3\,p\ ^4P^0_5-3\,d\ ^4D_3)$
4120.3	$\gamma\ (^3P)\ (3\,p\ ^4P^0_5-3\,d\ ^2F_5)$
4119.3	$\gamma\ (^1D)\ (3\,s\ ^2D_3-3\,p\ ^2P^0_1)$
4119.2	$\gamma\ (^3P)\ (3\,p\ ^4P^0_5-3\,d\ ^4D_7)$
4112 0	$\gamma\ (^3P)\ (3\,p\ ^4P^0_5-3\,d\ ^4D_5)$
4094.2	$\gamma\ (^3P)\ (3\,p\ ^4D^0_5-3\,d\ ^4F_3)$
4092.9	$\gamma\ (^3P)\ (3\,p\ ^4D^0_7-3\,d\ ^4F_7)$
4089,3	
4075.9	$\gamma\ (^3P)\ (3\,p\ ^4D^0_7-3\,d\ ^4F_9)$
4072.2	$\gamma\ (^3P)\ (3\,p\ ^4D^0_5-3\,d\ ^4F_7)$
4062.9	$\gamma\ (^3P)\ (3\,d\ ^4F_9-4\,f\ ^4F^0_9)$
4048.2	$\gamma\ (^3P)\ (3\,d\ ^4F_7-4\,f\ ^4F^0_7)$
3982.7	$\gamma\ (^3P)\ (3\,s\ ^2P_3-3\,p\ ^2P^0_1)$
3973.3	$\gamma\ (^3P)\ (3\,s\ ^2P_3-3\,p\ ^2P^0_3)$
3954.4	$\gamma\ (^3P)\ (3\,s\ ^2P_1-3\,p\ ^2P^0_1)$
3954.6	
3945.0	$\gamma\ (^3P)\ (3\,s\ ^2P_1-3\,p\ ^2P^0_3)$
3919.3	$\gamma\ (^1D)\ (3\,s\ ^2D_3-3\,p\ ^2P^0_1)$
3912.1	$\gamma\ (^1D)\ (3\,s\ ^2D_3-3\,p\ ^2P^0_3)$
3907.5	
3883.2	$\gamma\ (^3P)\ (3\,p\ ^4D^0_7-3\,d\ ^2F_5)$
3875.8	$\gamma\ (^3P)\ (3\,p\ ^4D^0_7-3\,d\ ^4D_5)$
3872.5	$\gamma\ (^3P)\ (3\,p\ ^4D_3-3\,d\ ^4D_1)$
3857.2	$\gamma\ (^3P)\ (3\,p\ ^4D^0_5-3\,d\ ^4D_5)$
3821.7	$\gamma\ (^3P)\ (3\,p\ ^2P^0_1-4\,s\ ^2P_1)$
3803.1	$\gamma\ (^3P)\ (3\,p\ ^2P^0_3-4\,s\ ^2P_3)$
3749.5	$\gamma\ (^3P)\ (3\,s\ ^4P_5-3\,p\ ^4S^0_3)$
3727.3	$\gamma\ (^3P)\ (3\,s\ ^4P_3-3\,p\ ^4S^0_3)$
3727.8	$\delta\ (^4S^0_3-{}^2D^0_5)$
3725.1	$\delta\ (^4S^0_3-{}^2D^0_3)$
3712.8	$\gamma\ (^3P)\ (3\,s\ ^4P_1-3\,p\ ^4S^0_3)$
3470 4	$\gamma\ (^3P)\ (3\,p\ ^2D^0_3-4\,s\ ^2P_1)$
3287 6	$\gamma\ (^3P)\ (3\,p\ ^4P^0_5-4\,s\ ^4P_5)$
3129.4	$\gamma\ (^3P)\ (3\,p\ ^4D^0_3-4\,s\ ^4P_3)$

OIII	
5006.9	$\gamma\ (^3P_2-{}^1D_2)$
4959.0	$\gamma\ (^3P_1-{}^1D_2)$
4363	$\gamma\ (^1D_2-{}^1S_0)$
3961.6	$\beta\ (3\,s\ ^1P^0_1-3\,p\ ^4S_0)$
3774	$\beta\ (3\,s\ ^3P^0_1-3\,p\ ^3D_1)$
3754.7	$\beta\ (3\,s\ ^3P^0_1-3\,p\ ^3D_2)$
3715.1	$\beta\ (3\,p\ ^3P_2-3\,d\ ^3D^0_3)$
3428.7	$\beta\ (3\,p\ ^3P_1-3\,d\ ^3P^0_2)$
3340.7	$\beta\ (3\,s\ ^3P^0_2-3\,p\ ^3S_1)$
3284.6	$\beta\ (3\,p\ ^3D_3-3\,d\ ^3F^0_3)$

On account of the great interest attached to the presence of these atomic lines in a luminescence emitted from the ionosphere, we have as far as possible given, for each line, the spectroscopic symbols for the electronic levels between which the atomic transition resulting in the line considered takes place.

This classification of the lines will be useful for the further discussion of the interpretation of of the lines appearing in the auroral spectrum.

Table VIII. *Atomic Nitrogen.*

NI	
λ	Classification
6441.7	$\gamma\,(^3P)\,(3\,p\,{}^4D^0_7 - 4\,d\,{}^4P_5)$
5999.5	$\gamma\,(^3P)\,(3\,p\,{}^2S^0_1 - 4\,d\,{}^2P_1)$
5829.5	$\gamma\,(^3P)\,(3\,p\,{}^4P^0_5 - 6\,s\,{}^4P_5)$
5616.5	$\gamma\,(^3P)\,(3\,p\,{}^4D^0_7 - 6\,s\,{}^4P_5)$
5328.7	$2\,s\,2\,p^4\,{}^4P_5 - \gamma\,(^3P)\,4\,p\,{}^4D^0_7$
(5200.8)	$\delta\,(^4S^0_3 - {}^2D^0_5)$
(5197.7)	$\delta\,(^4S^0_3 - {}^2D^0_3)$
4935.0	$\gamma\,(^3P)\,(3\,s\,{}^2P_3 - 4\,p\,{}^2S^0_1)$
4914.9	$\gamma\,(^3P)\,(3\,s\,{}^2P_1 - 4\,p\,{}^2S^0_1)$
4488.2	
4484.4	$2\,s\,2\,p^4\,{}^4P_1 - \gamma\,(^3P)\,4\,d\,{}^4P_5$
4336.5	
4305.5	
4223.0	$\gamma\,(^3P)\,(3\,s\,{}^4P_5 - 4\,p\,{}^4P^0_5)$
4114.0	$\gamma\,(^3P)\,3\,s\,{}^2P_3 - \gamma\,(^1D)\,3\,p\,{}^2D^0_3)$
3822.1	$\gamma\,(^3P)\,3\,s\,{}^2P_1 - \gamma\,(^1D)\,3\,p\,{}^2P^0_1)$
(3466.5)	$\delta\,(^4S^0_3 - {}^2P^0_{1\cdot 3})$

NII	
λ	Classification
6610.6	
6584 0	$\beta\,(3\,d\,{}^3D^0_3 - 4\,p\,{}^3D_2)$
6583.2	$\gamma\,(^3P_2 - {}^1D_2)$
6547.0	$\gamma\,(^3P_1 - {}^1D_2)$
6547.0	$\beta\,(3\,d\,{}^3D^0_1 - 4\,p\,{}^3D_1)$
6525.6	$\beta\,(3\,d\,{}^3D^0_1 - 4\,p\,{}^3D_2)$
5962	$\beta\,(3\,p\,{}^3P_2 - 3\,d\,{}^3D^0_1)$
5767.4	$\beta\,(3\,s\,{}^1P^0_1 - 3\,p\,{}^3D_1)$
5754.8	$\gamma\,(^1D_2 - {}^1S_0)$
5747.3	$\beta\,(3\,s\,{}^1P^0_1 - 3\,p\,{}^3D_2)$
5679.5	$\beta\,(3\,s\,{}^3P^0_2 - 3\,p\,{}^3D_3)$
5676.0	$\beta\,(3\,s\,{}^3P^0_0 - 3\,p\,{}^3D_1)$
5478.1	$\beta\,(3\,p\,{}^3P_1 - 3\,d\,{}^3P^0_2)$
5462.6	$\beta\,(3\,p\,{}^3P_1 - 3\,d\,{}^3P^0_1)$
5454.3	$\beta\,(3\,p\,{}^3P_1 - 3\,d\,{}^3P^0_0)$
5045.1	$\beta\,(3\,s\,{}^3P^0_2 - 3\,p\,{}^3S_1)$
4987.4	$\beta\,(3\,p\,{}^3S_1 - 3\,d\,{}^3P^0_0)$
4810.3	$\beta\,(3\,p\,{}^3D_3 - 3\,d\,{}^3D^0_2)$
4793.7	$\beta\,(3\,p\,{}^3D_2 - 3\,d\,{}^3D^0_1)$
4788.1	$\beta\,(3\,p\,{}^3D_2 - 3\,d\,{}^3D^0_2)$
4784	
4781.2	$\beta\,(3\,p\,{}^3D_2 - 3\,d\,{}^3D^0_3)$
4779.4	$\beta\,(3\,p\,{}^3D_1 - 3\,d\,{}^3D^0_1)$
4774.2	$\beta\,(3\,p\,{}^3D_1 - 3\,d\,{}^3D^0_2)$
4630.6	$\beta\,(3\,s\,{}^3P^0_2 - 3\,p\,{}^3P_2)$
4621.4	$\beta\,(3\,s\,{}^3P^0_1 - 3\,p\,{}^3P_0)$
4564.8	$\beta\,(3\,p\,{}^1D_2 - 3\,d\,{}^3F^0_2)$
4507.6	$\beta\,(3\,p\,{}^3D_3 - 3\,d\,{}^3P^0_2)$
4432.7	
4236.9	
4227.8	$\beta\,(3\,p\,{}^1P_1 - 4\,s\,{}^1P^0_1)$
4176.2	
4043.5	
4041.3	
4026.0	
3995.0	
3955.9	$\beta\,(3\,s\,{}^3P^0_1 - 3\,p\,{}^1P_1)$
3855.1	$\beta\,(3\,p\,{}^3P_1 - 4\,s\,{}^3P^0_0)$
3070.2	$\gamma\,(^3P_2 - {}^1S_0)$

NIII	
λ	Classification
6466.9	$\alpha\,(3\,p\,{}^4P_5 - 3\,d\,{}^4P^0_7)$
4634.2	$2\,s^2\,(3\,p\,{}^4P^0_5 - 3\,d\,{}^2D_3)$
4534.6	$\alpha\,(3\,s\,{}^4P^0_5 - 3\,p\,{}^4D_5)$
4530.8	$\alpha\,(3\,s\,{}^4P^0_3 - 3\,p\,{}^4D_1)$
4514.9	$\alpha\,(3\,s\,{}^4P^0_5 - 3\,p\,{}^4D_7)$
4510.8	$\alpha\begin{bmatrix} 3\,s\,{}^4P^0_1 - 3\,p\,{}^4D_3 \\ 3\,s\,{}^4P^0_3 - 3\,p\,{}^4D_5 \end{bmatrix}$
4379.1	$3\,s^2\,(4\,f\,{}^2F^0_{5\cdot 7} - 5\,g\,{}^2G_{7\cdot 9})$
4200.0	$3\,s^2\,(4\,p\,{}^2P^0_3 - 5\,s\,{}^2S_1)$
3754.6	$\alpha\,(3\,s\,{}^4P^0_3 - 3\,p\,{}^4S_3)$
3374.0	$\alpha\,(3\,s\,{}^4P^0_5 - 3\,p\,{}^4P_3)$
3367.3	$\alpha\,(3\,s\,{}^4P^0_5 - 3\,p\,{}^4P_5)$

In the case of OII, NI and NIII we have in Table VII and VIII written (n) instead of $\left(\frac{n}{2}\right)$ for the index expressing the quantnumber (j).

CHAPTER III.

On the Origin of the yellow Sodium Line in Twilight and in the Luminescence of the Night Sky and Aurorae.

§ 11. Introductory Remarks.

As is well known, the yellow sodium line is a doublet consisting of the two components D_1 (5895.52) and D_2 (5889.95). With spectographs of small dispersion the doublet appears as a single line with an apparent wave-length 5892.5.

That a yellow line with this wave-length is emitted from an atmospheric luminescence, was probably first observed by Slipher (22) in the night sky spectrum. A few years later the yellow line was observed in the light from the night sky, e. g. by Dufay (23), Vegard and Tønsberg (20), and by Sommer (24).

The appearance of the sodium line in the auroral luminescence was first observed by Vegard from spectrograms obtained at Tromsø 1932 (12). Since then the sodium line has been obtained with varying relative intensity on a large number of auroral spectrograms (6, 16), compare also Pl. I of this paper.

Dufay in 1932 was the first to notice the fact that the yellow line in the night sky luminescence had a wave-length equal to that shown by the sodium doublet (D_1D_2), taken with spectrographs with a dispersion too small for the separation of the components. From the variation of its intensity with the zenith distance he showed that the yellow line was of atmospheric origin.

In 1936 Vegard found that the intensity of the red triplet and the negative nitrogen bands relative to that of the green line is considerably enhanced when the auroral luminescence is emitted from an atmosphere exposed to sunlight.

In the same year some spectrograms of twilight were taken by Vegard and Tønsberg at Oslo and at Tromsø. In spite of the short exposure of a few minutes, the spectrograms showed the yellow sodium line (5892) very distinctly (6, 16). It may be roughly estimated that in order to obtain the yellow line with the same photographic density the time of exposure must be about a hundred times longer in the case of the light from the night sky. This means that the sodium line which appears in the night sky luminescence *is enormously enhanced when the atmosphere is exposed to sunlight.*

Vegard, who considered it rather unlikely that lines from sodium were emitted from the upper atmosphere, suggested as a possible interpretation that the line was a narrow band belonging to the first positive group of nitrogen. In order to find out whether the yellow line ought to be referred to sodium Bernard (25, 27) in 1938 and at about the same time Cabannes, Dufay, and Gauzit (30) analysed the fine structure of the line by means of a Fabry-Perot interferometer. They showed that the line consisted of two components having a wavelength difference equal to that of the two components D_1 and D_2 of sodium.

In 1939 Vegard and Tønsberg, using a big glass spectrograph with a dispersion sufficient for the the separation of the two components, showed that the yellow line was indeed identical with the D_1D_2 doublet, both as regards the wave-length and the relative intensity of the components (16).

In December 1935 and January 1936 Garrigue at Pic-du-Midi (39) determined the intensity of the yellow line in the night sky luminescence in the zenith (B_Z) and near the horizon (B_H). On the assumption that the sodium line originates from a comparatively thin layer somewhere in the atmosphere Cabannes, Dufay, and Gauzit tried to determine the height H of this layer from the intensity ratio B_H/B_Z. On certain assumptions they found $H = 130$ km, and they assume that the yellow radiation in the night sky is a luminescent phenomenon accompanying the fall of the meteorites. As pointed out by Bernard (28), this determination of H is most uncertain and open to criticism. The assumption that the sodium light from the night sky is restricted to a fairly thin layer hardly corresponds to real facts, and secondly, the intensity ration B_H/B_Z is very difficult to measure accurately, — and comparatively small errors have a large influence on the altitude H of the sodium layer.

During the winter 1937—1938 Bernard made observations of the yellow line in the twilight spectrum at the Auroral Observatory, Tromsø. He took series of spectrograms of the twilight luminescence and showed that the intensity of the yellow line dropped off quite suddenly. He determines the time when the line disappears on his spectrograms. At this moment the point where the collimator axis cuts the shadow limit produced by the *surface of the earth* is situated at a certain altitude H_u which is easily calculated. Bernard finds that H_u on an average is about 60 km, and assuming that the yellow sodium line is excited by the ordinary sunlight through a resonance effect, Bernard arrives at the conclusion that the yellow sodium line is emitted from an atmospheric layer which has its upper limit about 60 km above the ground.

Having thus found that the emission of the (D_1D_2)-doublet in twilight is mainly restricted to a layer below 60 km, he advocates the view that the sodium is of terrestrial origin (27, 28). He assumes that "salt particles from the oceans are carried up by ascending currents to very great altitudes, where their vaporation gives rise to NaCl molecules capable of being dissociated under certain influences" (29).

In 1939 series of twilight spectrograms were taken both at Oslo and at Tromsø with the object of determining the moment at which the intensity of the D-line drops down to be quite insignificant. The results were published by Vegard and Tønsberg in 1940 (16).

When the weather permitted, a series was first taken towards the zenith, then the collimator was directed towards the twilight near the horizon with an azimuth equal to that of the sun, and a new series was taken. According to the view advocated by Bernard that the sodium D-doublet is excited by ordinary sunlight, the upper limit of the D-emission would be determined by the shadow of the solid earth. On the basis of this assumption Vegard found that the observations near the horizon gave a greater upper limit

(H_u) for the effective emission layer than the zenith observations.

Assuming, however, that the D-line is excited by some easily observed — ultraviolet — solar radiation, and that the atmosphere below a certain height (H_s) acts as a screen for the effective solar rays, this "*screening height*" *was found from the condition that spectra from the zenith and those taken in a direction towards the western horizon give the same upper limit* (*H_u*) *for the D-emission in twilight* (34).

To a given elevation α of the collimator axis we can find the upper limit (H_a) corresponding to any given value of the screening height (a), or we can determine the function

$$H_a^\alpha = f_\alpha\ (a)$$

The curve representing this function is nearly a straight line, and the point (H_1, a_1) where the zenith curve cuts the horizon curve gives us the true value of the screening height ($H_s = a_1$) and the upper limit of twilight D-emission ($H_u = H_1$).

The values of H_u) and (H_s) found from the Oslo and Tromsø observations are given in Table IX.

Table IX.

	Hs	Hu
Oslo	58 km	119 km
Tromsø...	50 »	109 »
Mean	54 km	114 km

The screening effect of the atmosphere below the screening height was explained by the assumption that the effective solar radiation consists of ultraviolet light mainly in the interval 1950—3000 Å which is strongly absorbed by atmospheric ozone. This was found to be in good agreement with the fact that the screening height is considerably greater than the height at which the ozone concentration has its maximum.

Thus with respect to the excitation of the D-radiation there is a kind of twilight phenomen determined by the "ozone shadow" with reference to the ultra-violet region of the solar spectrum. We might call it the "uviol twilight" or "uviol dawn" produced by the atmospheric ozone.

In a paper published in 1943 Penndorf (33) gives results of calculations of the shadow limit produced by ozone on ultra-violet light, on varying assumptions regarding the rate of diminution of the ozone concentration and the absorption coefficients of the ultra-violet light. He finds that the theoretical results are in good agreement with the screening height found by Vegard and Tønsberg (16).

This result involves that the ozone concentration must be extremely small above the screening height, a result which has important consequences for the physics of the ionosphere and the interpretation of the auroral spectrum. An exact determination of the screening height (H_s) and of the upper limit (H_u) of the twilight D-emission is therefore a matter of great interest in connection with the study of the distribution of ozone in the atmosphere and for the study of the origin and excitation of the sodium in the atmosphere.

As already mentioned, the determination of (H_s) and (H_u) is based on the determination of the time (τ) when the twilight D-emission disappears in a certain part of the sky. By the determination of (τ) we have followed the method first used by Bernard at the Tromsø auroral observatory.

With the collimator of the spectrograph put in a certain direction in the vertical plane through the sun, we take a series of spectrograms and continue until one of the spectrograms covers the time interval within which the twilight D-emission disappears. From the way in which the density of the sodium line varies within the series of spectrograms we may estimate fairly accurately the point of time (τ).

In the case of the observations treated by Vegard and Tønsberg in the paper referred to (16), the value of (τ) was found in that way. In order to increase the accuracy of (H_s) and (H_u), we have here adopted a method based on photometric measurements of the intensity of the sodium line for each series of spectrograms. Our procedure will be dealt with later on.

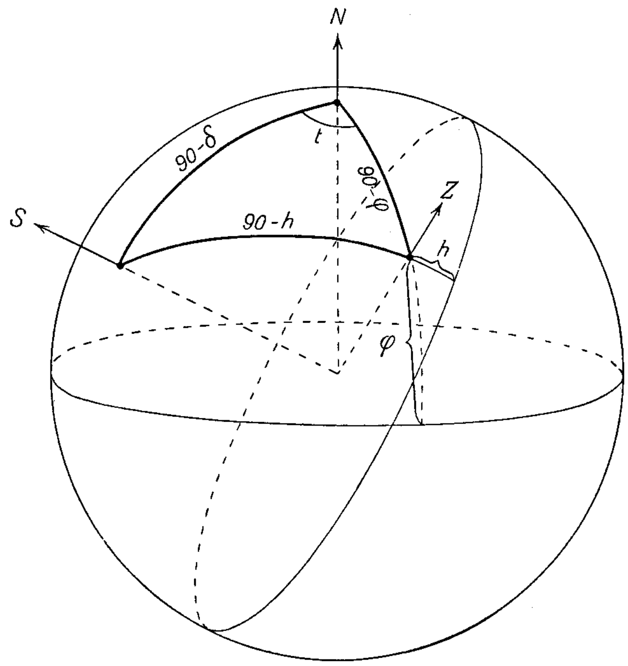

Fig. 2.

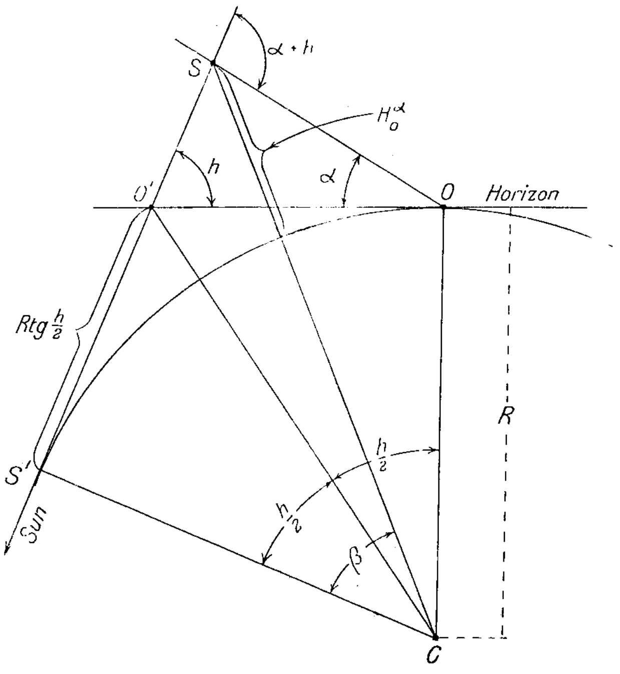

Fig. 3.

§ 12. On the Determination of the Relation between (H) and (*a*) at a given Moment and with a given Direction of the Collimator Axis.

The moment (τ) for which the relation between (H) and (*a*) is to be found, is supposed to be given in mean European time reckoned from noon. The hour angle (t) of the sun has then to be calculated from the formula

$$t = 15\,(\tau - 1 + \Delta) + \lambda \tag{1}$$

The time equation Δ is found from the Nautical Almanac.

λ is the longitude (E. Gr.) of the spot of observation. In the case of Oslo we have

$$\lambda = 10^\circ.72, \quad \varphi = 59^\circ.95.$$

The height of the sun (h) corresponding to a known hour angle (t) is found from the spherical triangle (Fig. 2) by means of the equation:

$$\sin h = \sin \delta \sin \varphi + \cos \delta \cos \varphi \cos t. \tag{2}$$

δ = sun's declination, which is taken from the Nautical Almanac.

In Fig. 3 the plane of the paper represents a vertical plane through the spot of ohservation, the collimator axis, and the sun. OO′ is the horizon, OS the collimator axis forming an angle α with the horizon, and SS′ the shadow limit of the sun's radiation produced by the surface of the earth, the radius of which is denoted by R.

We want to find the height (H_0^α) of the point (S) where the collimator axis cuts the shadow line.

From the triangle OSO′ we get:

$$\frac{x}{\sin \alpha} = \frac{R \operatorname{tg} \frac{h_\alpha}{2}}{\sin(\alpha + h_\alpha)} \tag{3}$$

and from the triangle CSS′

$$\operatorname{tg} \beta = \frac{x + R \operatorname{tg} \frac{h_\alpha}{2}}{R}$$

Inserting x from equation (3):

$$\operatorname{tg} \beta = 2 \frac{\sin \frac{h_\alpha}{2} \sin\left(\alpha + \frac{h_\alpha}{2}\right)}{\sin(\alpha + h_\alpha)} \tag{4}$$

and

$$H_o^\alpha = R\left(\frac{1}{\cos \beta} - 1\right) \tag{5 a}$$

When the collimator is directed towards zenith, $\alpha = 90^\circ$, $\beta = h$, and

$$H_o^z = R\left(\frac{1}{\cos h_z} - 1\right) \tag{5 b}$$

The case where the atmosphere up to a certain height (a) acts as a screen to the effective solar radiation is illustrated in Fig. 4. The altitude H_a^α of the point where the collimator axis cuts the atmospheric shadow line is now given by the equation:

$$\mathrm{H}_a^\alpha = \frac{a}{\cos\gamma_1} + \mathrm{R}\left(\frac{1}{\cos\gamma_1} - 1\right) \tag{6 a}$$

Where:

$$\operatorname{tg}\gamma = \frac{\mathrm{z}-\mathrm{j}}{\mathrm{R}+a} = \frac{1}{\mathrm{R}+a}(\mathrm{R}\operatorname{tg}\beta - a\operatorname{cotg}(\alpha+\mathrm{h}_a))$$

or putting $a/\mathrm{R}=\varepsilon$:

$$\operatorname{tg}\gamma = \frac{1}{1+\varepsilon}\operatorname{tg}\beta - \frac{\varepsilon}{1+\varepsilon}\operatorname{cotg}(\alpha+\mathrm{h}_\alpha) \tag{7}$$

As ε is a very small quantity the angle γ differs very little from β — which is independent of (α). Thus according to equation (6) the height (H_a^α) is nearly a linear function of the screening height (a).

In the case of the zenith observations we have $\alpha=90°$, $\gamma=\beta=\mathrm{h}$, and

$$\mathrm{H}_a^z = \mathrm{R}\left(\frac{1}{\cos\mathrm{h}_z} - 1\right) + \frac{a}{\cos\mathrm{h}_z}$$

$$\mathrm{H}_a^z = \mathrm{H}_o^z + \frac{a}{\cos\mathrm{h}_z} \tag{6 b}$$

When the atmospheric refraction is not taken into account, (H_a^z) is a linear function of a.

The screening height which interests us is the one (a_1) which makes the upper limit of the D-emission at the zenith (H_u^z) equal to the upper limit near the horizon ($\mathrm{H}_\mathrm{u}^\alpha$). As already mentioned, this value of a_1 is about 50 km and for altitudes higher than about 25 km the refraction is too small to have any essential influence on our results.

In order to determine the curve $\mathrm{H}_a = \mathrm{f}(a)$ for the zenith observations and for the observations near the horizon, we may, for instance, calculate the the values of H_a^z and H_a^α for $a=25$, 50, 100, and 150 km, for which the atmospheric refraction can be omitted.

The point of intersection between the two curves gives us the true screening height ($a_1=\mathrm{H}_\mathrm{s}$) and the true upper limit of D-emission ($\mathrm{H}_a^\alpha=\mathrm{H}_\mathrm{u}$).

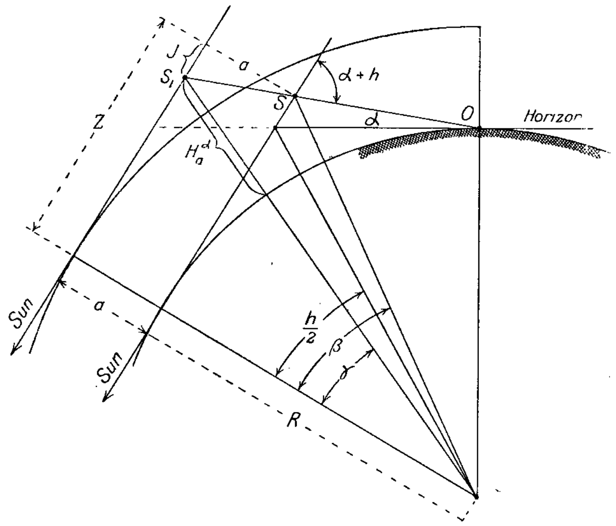

Fig. 4.

The values of H_u and H_s can also be found by direct calculation. From equations (6 a) and (6 b) we get:

$$\mathrm{H}_{a_1}^\alpha = \frac{a_1}{\cos\gamma_1} + \mathrm{R}\left(\frac{1}{\cos\gamma_1} - 1\right) = \mathrm{H}_{a_1}^z = \frac{a_1}{\cos\mathrm{h}_z} + \mathrm{R}\left(\frac{1}{\cos\mathrm{h}_z} - 1\right)$$

which reduces to

$$\cos\gamma_1 = \cos\mathrm{h}_z$$

or

$$\gamma_1 = \mathrm{h}_z \tag{8}$$

This inserted into equation (7) gives

$$\operatorname{tg}\mathrm{h}_z = \frac{\mathrm{R}}{\mathrm{R}+a_1}\operatorname{tg}\beta - \frac{a_1}{\mathrm{R}+a_1}\operatorname{cotg}(\alpha+\mathrm{h}_\alpha)$$

and

$$a_1 = \mathrm{H}_\mathrm{s} = \mathrm{R}\frac{\operatorname{tg}\beta - \operatorname{tg}\mathrm{h}_z}{\operatorname{tg}\mathrm{h}_z + \operatorname{cotg}(\alpha+\mathrm{h}_\alpha)} \tag{9 a}$$

Inserting the expression for $\operatorname{tg}\beta$ (equation 4):

$$\mathrm{H}_\mathrm{s} = \mathrm{R}\frac{2\sin\frac{\mathrm{h}^\alpha}{2}\sin\left(\alpha+\frac{\mathrm{h}_\alpha}{2}\right) - \operatorname{tg}\mathrm{h}_z\sin(\alpha+\mathrm{h}_\alpha)}{\operatorname{tg}\mathrm{h}_z\sin(\alpha+\mathrm{h}_\alpha) + \cos(\alpha+\mathrm{h}_\alpha)}$$

or

$$\mathrm{H}_\mathrm{s} = \mathrm{R}\frac{2\cos\mathrm{h}_z\sin\frac{\mathrm{h}_\alpha}{2}\sin\left(\alpha+\frac{\mathrm{h}_\alpha}{2}\right) - \sin\mathrm{h}_z\sin(\alpha+\mathrm{h}_\alpha)}{\cos(\alpha+\mathrm{h}_\alpha-\mathrm{h}_z)} \tag{9 b}$$

The upper limit of D-emission (H_u) is found from equation (6 b) by putting $a = H_s$:

$$H_u = \frac{R + H_s}{\cos h_z} - R \tag{10}$$

By means of the equations (9) and (10) the screening height (H_s) and the upper limit of the twilight D-emission (H_u) can be calculated directly from the observed or known quantities.

The quantities (H_s) and (H_u) can also be found in a quite convenient way by means of equation (8). The angle (γ) is calculated for a number of a-values in the neighbourhood of H_s, and the value of (a) which makes $\gamma = h_z$ (and which is equal to H_s) can be found either graphically or by interpolation.

§ 13. On the Determination of the Time of Disappearance of the D-line in Twilight.

A number of twilight spectra 1, 2, . . . i, . . . n are taken on the same photographic plate, which also contains an intensity scale.

Let the exposure times of the spectra be $t_1, t_2, \dots t_i, \dots t_n$. From the intensity scale we construct a curve which gives the photographic density as a function of the deflection (u) of the galvanometer connected to the registering spectrophotometer.

The total photographic density (W_i) of the D-line on one of the spectrograms (i) is the sum of that due to the D-line and that caused by the continuous spectrum. Then according to the law of Schwarzschild

$$(I_d + I_c)_i\, t_i^p = W_i' = \varphi(u_i')$$

I_d and I_c are the intensities of the D-line and of the continuous spectrum close to it. u_i' is the total galvanometer deflection of the D-line, and W_i' the corresponding density taken from the curve constructed by means of the intensity scale.

The mean deflection (u_i'') due to the continuous spectrum on both sides of the D-line is found from the photometer curve in the way indicated in Fig. 5. Then:

$$(I_c)_i\, t_i^p = W_i'' = \varphi(u_i'')$$

The intensity of the D-line measured in an arbitrary unit, which however is the same for the whole spectral series, is found from the equation:

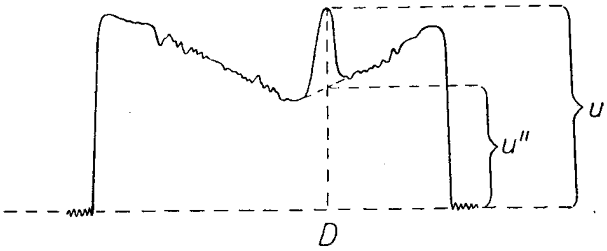

Fig. 5.

$$(I_d)_i = \frac{\varphi(u_i') - \varphi(u_i'')}{t_i^p} = \frac{S_i}{t_i^p} \tag{11}$$

The Schwarzschild constant (p) is equal to about 0.9, but for our purpose it appears that we may put $p = 1$.

In order to find the time (τ) when the D-emission in the twilight practically stops, we draw a curve with the time as abscisse and the intensities (I_d) calculated from equation (11) as ordinates. The procedure is illustrated in Fig. 6 a and b.

By constructing the curve Fig. 6 the intensity (I_d) found for each of the spectrograms is as a rule drawn from the midst of the exposure interval. The last spectrogram on which the D-line appears requires special treatment. In this case the point of time (τ) at which D-emission vanishes is situated somewhere within the exposure interval, and only a fraction of the exposure interval contributes to the photographic density of the D-line.

Our problem is to determine (τ) from the intensity curve constructed by means of the spectrograms and from the density of the D-line on the last spectrogram. For this purpose we have been using two different methods: One we might call " the graphical method of gradual approximation " and the other is " a method of direct calculation of (τ) ".

a. *The Graphical Method of Gradual Approximation.*

Let the last spectrogram on which the D-line appears be denoted by (n) and the exposure interval by (t_n). Suppose the D-line disappeared just at the end of this interval, then we might suppose that the intensity of the D-line during the exposure t_n decreases in a linear way from an intensity (j) to zero. We calculate an intensity (I_n) by putting t_n in equation (11).

In the graphic represention Fig. 6 we do not draw I_n from the midst of the exposure interval

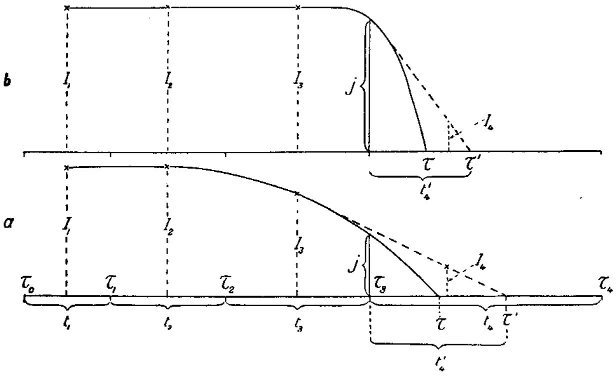

Fig. 6.

(t_n), but the most reasonable procedure would be to draw it from a point determined by the condition that it divides the interval in such a way that the light sum $\Sigma I \Delta t$ is the same on both sides. This means that we should draw the intensity (I_n) from a point situated at a distance equal to $\frac{t_n}{\sqrt{2}}$ from the end of the exposure interval. For the sake of convenience, however, we have preferred to draw (I_n) from a point at a distance $^2/_3\, t_n$ from the end of the interval.

The intensity curve drawn through the point thus found (Fig. 6) cuts the abscisse at a point (τ') and determines a new effective exposure interval (t_n'). This introduced into equation (11) gives a new and greater intensity (I_n'). If this intensity drawn from a point at a distance of $^2/_3\, t_n'$ from (τ') just ends on the intensity curve already drawn, the process stops and (τ') will give us the point of time when the D-emission vanishes. If the curve drawn through the upper end of the intensity line (I_n') falls below the previous curve it determines a new stopping point (τ'') and a new intensity I_n'', and the process is continued until (τ), and the effective exposure interval, is reduced to a minimum and the process stops automatically. As a rule one or two steps brings us to the final value of (τ).

b. The Method of direct Calculation.

The photographic density (S_n) of the D-line on the last spectrogram is produced by light with an intensity which gradually decreases from (j) at the beginning of the exposure and becomes zero after a time Δt. If the exposure begins at an hour (τ_{n-1}) then the stopping hour (τ) of the sodium line will be:

$$\tau = \tau_{n-1} + \Delta t \tag{12}$$

Δt has to be calculated from the equation:

$$\int_0^{\Delta t} I\, dt = S_n \tag{13}$$

If the intensity curve has been gradually falling before the beginning of the last exposure, we may assume the intensity to be a linear function of time, or:

$$I = j\left(1 - \frac{t}{\Delta t}\right) \tag{14 a}$$

and from equation (13):

$$\Delta t = \frac{2\, S_n}{j} \tag{15 a}$$

The point of time (τ) when the D-emission stops is found from equation (12). The density (S_n) is determined by photometry and (j) is found from the intensity curve as it is fixed by the whole series of spectrograms.

If the intensity of the D-light keeps nearly constant until it suddenly drops during the exposure of the last spectrogram, we may as a first approximatiou assume, that the last part of the curve is a parabola expressed by the equation:

$$I = j\left[1 - \left(\frac{t}{\Delta t}\right)^2\right] \tag{14 b}$$

This value of I introduced into equation (13) gives:

$$\Delta t = \frac{3}{2}\, \frac{S_n}{j} \tag{15 b}$$

In most cases the intensity curve is of the type (a) Fig. 6 and Δt can be calculated from equation (15 a).

§ 14. Observations and Results.

During the winter season 1942—43 21 series of successful twilight spectrograms were taken in the zenith direction, and 24 with the collimator directed at an elevation $\alpha = 10^\circ$ above the horizon. In order to see whether the screening height (H_s) and the upper limit (H_u) might possibly vary with the season of the year, we divided the observations into two groups, one containing the spectral series taken from Oct. 9, 1942 to Febr. 13, 1943, and a second

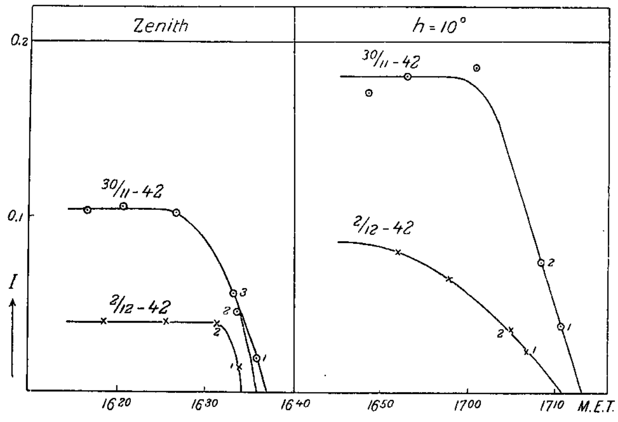

Fig. 7 a.

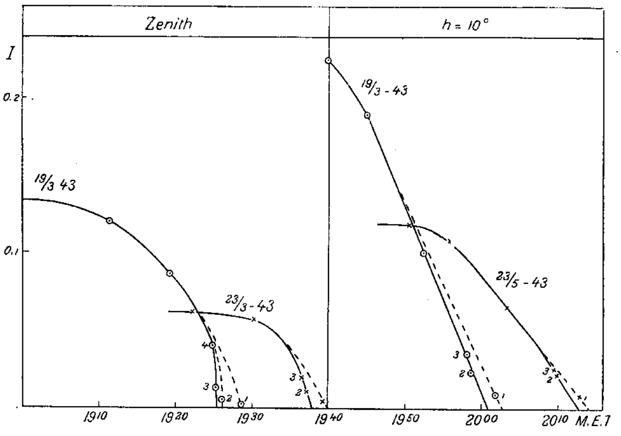

Fig. 7 b.

one containing about an equally great number of spectral series taken from Febr. 18 to April 15, 1943.

By way of illustration spectral series of 4 evenings, two from each of the two groups, are reproduced on Pl. III. Each evening we commence with a zenith-series, then follows one from near the horizon. ($\alpha = 10^\circ$).

The corresponding intensity curves are shown in Figs. 7 a and 7 b. These curves serve to illustrate the fluctuation of the intensity of the D-emission from one evening to another, and also to illustrate the graphical method for determining the time of disappearance of the D-line by gradual approximation. The points found by the first, second, and third step are denoted by Figures 1, 2, 3, etc.

The curves show that during the same evening the intensities from the zenith are considerably smaller than those from near the horizon.

On November 30, 1942 the intensities are considerably greater than the corresponding intensities on December 2, and they are greater on March 19, 1943 than a few days later, on March 23.

In the determination of the solar height (h) we have not always used the equation (2), as for our purpose we found it more convenient and sufficiently accurate to use the "Curves for solving a Spherical Triangle", by L. Becker of the University Observatory, Glasgow.

The solar heights at the moment (τ) of disappearance of the D-line in twilight are given in Tables (X_a) and (X_b), corresponding to the groups into which we divided our observations. The table gives for each evening the date, the moment (τ) of the disappearance of the D-line, the hour angle (t), and the solar heights (h) for the observations towards the zenith and for those taken in a direction $\alpha = 10^\circ$ above the horizon.

The solar heights for zenith and also for the observations near the horizon show small, but quite irregular variations, which may be due to errors. We have therefore not calculated the screening height (H_s) and the upper limit of twilight D-emission (H_u) for each evening, but only for the mean solar heights given at the bottom of each of the two tables (X_a) and (X_b). The values of (H_s) and (H_u), calculated directly by means of the formulae (9) and (10), are given in Table (XI).

The different values of (H_s) and (H_u) shown by the two groups may be due to errors, and at the present time we do not feel justified in regarding this difference as indicating a real variation of these quantities.

As long as the exposure of the last spectrograms of a series amounts to as much as 10—15 minutes, the errors in the stopping time (τ) in somewhat unfavourable cases may amount to 2—3 minutes. In order to increase the accuracy it would be adventageous to reduce the time of exposure and increase the number of spectrograms giving the D-line with measurable intensity. This means that we have to use a spectrograph which combines a very great light power with a fairly great dispersion. Our spectrograph (C) which we have been using, fulfils these conditions in a fairly satisfactory way. Further, the observations ought to be taken at high latitudes with long duration of the twilight, and finally the observations for the

Table X.

The Hour of Disappearance (τ) of the Twilight D-emission and the corresponding Hour Angle (t) and Height of the Sun.

Date	τ (M. E. T.)		*t* (at Oslo)		h	
	Zenith	Horizon $\alpha = 10°$	Zenith	Horizon $\alpha = 10°$	Zenith	Horizon $\alpha = 10°$
a. *Group of Observations from 9/10 1942—13/2 1943.*						
1942	h m	h m				
9/10		19 01		104°.10		—12°.50
16/10		18 40		99°.35		—12°.45
17/10	18 04	18 37	90°.35	98°.60	—8°.05	--12°.35
19/10	17 58	18 32	88°.97	97°.47	—8°.00	—12°,37
27/10		18 12		92°.72		—12°.37
16/11	16 52	17 29	72°.47	81°.72	—7°.78	—12°.20
23/11	16 43		69°.72		—7°.88	
29/11		17 15½		77°.47		—12°.45
30/11	16 36	17 13	67°.47	76°.85	—8°.00	—12°.35
2/12	16 34½	17 11	66°.97	76°.23	—8°.10	—12°.33
30/12	16 35	17 15	63°.72	73°.85	—7°.82	—12°.33
1943						
8/1	16 46	17 24½	65°.72	75°.22	—7°.95	—12°.30
13/2	18 00	18 39	82°.15	91°.89	—7°.60	—12°.45
				Mean	—7°.91	– 12°.37
b. *Observations from 18/2—15/4, 1943.*						
1943	h m	h m				
18/2	18 14	18 46½	85°.72	93°.85	--8°.05	—12°.22
2/3	18 41	19 16	92°.85	101°.60	—7°.75	—12°.12
3/3	18 45	19 18	93° 97	102°.22	—7°.98	—12°.15
9/3	19 00	19 32½	97°.97	106°.22	—7°.92	—12°.12
11/3	19 03	19 38	98°.97	107°.72	—7°.75	—12°.22
12/3	19 07	19 41	99°.97	108°.47	—7°.98	—12°.22
19/3	19 25½	20 01	105°.10	113°.97	—8°.03	—12°.30
20/3	19 28½	20 04	105°.85	114°.72	--8°.05	—12°.30
23/3	19 36	20 11	107°.97	116°.72	– 7°.98	—12°.20
24/3	19 38	20 13	108°.47	117°.47	—7°.85	—12°.20
1/4	19 59	20 36	114°.47	123°.72	--7°.95	—12°.12
15/4	20 39½	21 23	125°.47	136°.47	--8°.00	—12°.22
				Mean	—7°.94	—12°.20

determination of (H_s) and (H_u) ought to be taken at times when the D-emission is comparatively strong. Comparing the results given in Table XI with those of Table IX, we notice that the values found for (H_s) and (H_u) from the Oslo observations dealt with in this paper are somewhat lower than those previously found from the observations at Oslo and Tromsø in 1939. This difference may — at any rate partly — be due to the more exact manner in which the D-emission was determined from the present observations.

Table XI.

	Group a 9/10 42— 13/2 43	Group b 18/2 —15/4 43	Mean
α	10°	10°	10°
h_z	—7°.91	—7°.94	—7°.93
h_α	—12°.37	—12°.20	—12°.29
H_s	46.8 km	40.5 km	43.7 km
H_u	108.3 km	102.5 km	105.4 km

Table XII.

	H_s	H_u
Oslo 1939.....	58 km	119 km
Tromsø 1939 ..	50 km	109 km
Oslo 1942—43.	46.8 km	108.3 km
Oslo 1943.....	40.5 km	102.5 km
Mean.........	48.8 km	109.7 km

The results hitherto obtained regarding the screening height and the height of the upper limit of the twilight D-emission are collected in Table XII.

Our results and those previously given by Vegard and Tønsberg are so far in good agreement, as they give a screening height (H_s) far above the height (25 km) at which the ozone concentration is a maximum, and the conclusions drawn from the previous results in Vegards and Tønsberg's papers regarding the type of solar radiation which excites the emission of the sodium D-line still hold good (16, 34).

The D-line is excited by the ultra-violet radiation of the sun and the atmospheric screening is produced by the atmospheric ozone which absorbs the effective ultra-violett solar radiation. *The D-emission is governed by the "uviol twilight" produced by the ozone in the atmosphere.*

§ 15. On the Origin and State of the Atmospheric Sodium.

Giving equal weight to all results in Table XII, it appears that the atmosphere below about 50 km acts as a screen to the effective solar radiation, and that the twilight D-emission nearly vanishes at an altitude of about 110 km. This result does not mean that twilight D-emission is absent above 110 km and that the effective ultra-violet sunlight produces no D-emission above this height. It only means that at an altitude of about 110 km the intensity of the D-line suddenly drops to such a small value that it would require exposures of a greater order of magnitude to get it on our photographic plates with the spectrographs used.

Assuming that the sodium D-line is excited by ordinary sunlight and that the surface of the solid earth acts as a screen to the effective solar radiation which is transmitted by the atmosphere above the ground, Bernard (27, 29) found that the D-emission stops at an altitude of about 60 km. He advocates the view that the sodium is of terrestrial origin and due to salt particles from the oceans, which are carried to great altitudes, "where their evaporation gives rise to NaCl molecules capable of being dissociated under certain influences". He suggests that the dissociation of the NaCl molecules is due to a high temperature existing in a thin layer at an altitude of 60 km. As we have seen, Bernards determination of the upper limit of D-emission is based on the erroneous assumption that the whole atmosphere is transparent to the effective solar radiation, and further we have no evidence for the existence in the stratosphere of a temperature sufficiently high to effect the dissociation of NaCl molecules.

As an argument in favour of his view of the terrestrial origin of the sodium in the atmosphere, he mentiones "the absence of sodium atoms in the auroral region". This argument, however, is not valid, for as shown in this and previous papers the sodium D-line appears with considerable intensity not only in the spectrum of the night sky, but also in that of the aurorae. We may in this connection refer to Chapter I of this paper and, for instances to spectrograms Nos. 29 and 30, on which the D-line appears with considerable intensity, although the spectrograms correspond to the upper limit of the aurora, and are taken in the middle of the night. Thus the appearance of the D-line in the auroral spectra has nothing to do with the twilight luminescence. The fact that the sodium line appears with such great intensity at the upper part of the aurora, is very remarkable, and it shows that the Na-concentration diminishes more slowly with the altitude than would have been the case if the distribution of matter in the auroral region had been governed by the barometric height formula applied to an atmosphere in equilibrium under the influence of gravitation only.

The slownes with which the sodium density diminishes upwards is, however, explained by Vegard's theory of the upper atmosphere, according to which atmospheric matter in a partly ionised state is driven upwards through the effect of electric forces produced by a radiation from the sun of the type of soft X-rays.

As already mentioned, Cabannes, Dufay, and Gauzit (30) advanced the hypothesis that the sodium originates from meteorites. The hypothesis has been criticized by Déjardin and Bernard. Their first argument against it is the absence of the sodium D-line in the auroral spectrum, and that according to Bernard's measurements the D-emission takes place below 60 km. These two arguments, however, are no longer valid.

As a third argument they mention that the amount of sodium in the meteorites is extremely small. In our opinion, however, the most weighty argument against the meteorite hypothesis is that the excitation of the sodium by ultra-violet light, and in the night sky luminescence, and probably also in the aurorae, requires that the sodium should exist in the form of some chemical compound, and the meteoric matter would probably exist mostly in the form of dust.

One of us advanced the hypotheses (15, 16, 32) that showers of sodium atoms, coming from the sun like those of hydrogen atoms, precipitate into the atmosphere. This hypothesis explains the presence and distribution of sodium in the auroral region, and the large and apparantly irregular fluctuations in the intensity of the D-line, while it introduces no difficulties as regards the excitation processes in twilight, in the night sky, and in the aurorae. As pointed out by one of us (15, 16, 32) the precipitation of hydrogen and sodium into the higher strata of the atmosphere may explain the formation of the luminous night clouds, which appear at an altitude of 80 km. The hydrogen and the sodium atoms combine with oxygen, and the sodium oxide provides very effective nuclei for the condensation of water vapour, so that the cloud may exist at the great altitude of 80 km.

Summary of Results.

1. The paper deals with 36 auroral spectrograms taken at Oslo, and most of them with a fairly great dispersion.
2. On some of the spectrograms the H_β line appears with an intensity even greater than that of the negative nitrogen band 4708. On other spectrograms taken on the same sort of plates where the negative bands are equally strong, the H_β line is much weaker than 4708, or absent. The spectrograms thus give new evidence for the great fluctuations of the hydrogen lines, indicating corresponding fluctuations in the hydrogen concentration within the auroral region due to streams of H-atoms or protons occasionally coming from the sun.
3. Similar fluctuations are found for the sodium D-line, which sometimes, even at the middle of the night, appear with considerable intensity in the auroral spectra corresponding to various altitudes.
4. On some of the spectrograms two lines, 6157 and 5993, which nearly coincide with bands of the 1st positive nitrogen group, appear isolated with considerable intensity, while other bands of the 1. P. G. are very weak or absent. This indicates that these lines are to be identificated with the OI-triplet (6158, 6157, 6156) and the OI-line 5995.
5. Spectrograms taken on “Agfa Spectral Blau Ultra rapid” plates, very sensitive in the blue and violet, show that a number of OII-lines are greatly enhanced with increasing altitude, showing that the relative concentration of O^{1+} ions increases with altitude.
6. Comparable spectrograms from the lower and upper limit of the aurorae taken on Agfa ISS panchromatic plates, show very clearly the enhancement relative to the green OI-line (5577) of the red OI doublet (6300, 6364) and of the bands of the negative nitrogen group with increasing altitude. These altitude effects, which were detected by Vegard, have also been dealt with in a number of previous papers.
7. An auroral spectrogram from a sunlit atmosphere showed the enhancement of the red OI doublet in accordance with previous observations.
8. Spectrograms of the negative bands from the lower and the upper limit of aurorae did not show any broadening of the R-branch with increase of the altitude. This means that at night the temperature of the ionosphere does not materially increase with increase of altitude.
9. The 173 auroral lines and bands hitherto observed and measured are given in a table containing wave-lengths, interpretations and results of intensity measurements.
10. A very great number of lines are referred to O- and N-atoms in various states of ionisation. The OI, OII, and OIII lines and those from NI, NII, and NIII which may possibly appear in the auroral luminescence are collected in separate tables. For most of these lines the tables also give the spectroscopic classification or the symbols of the states which are engaged in the emission of the lines.
11. The appearance of the sodium D-line in twilight has been studied by means of series of spectrograms taken at the zenith and in a direction $\alpha = 10^\circ$ above the horizon.
12. The intensity variation of the D-line within each series of spectrograms was determined photometrically, and two methods are given for the determination of the point of time (τ) when the D-emission vanishes.
13. The height of the sun corresponding to the time (τ) is calculated for the zenith observations (h_z) and for the observations near the horizon (h_α).
14. Following the results given in a previous paper by Vegard and Tønsberg, to the effect that the D-line is excited by ultra-violet light and that a layer of the atmosphere below a certain height (H_s) acts as a screen to the ultra-violet light, the following formulae for

direct calculation of the screening height (H_s) and the upper limit of the D-emission (H_u) are given:

$$H_s = R \frac{2 \cos h_z \sin \frac{h_\alpha}{2} \sin\left(\alpha + \frac{h_\alpha}{2}\right) - \sin h_z \sin(\alpha + h_z)}{\cos(\alpha + h_\alpha - h_z)}$$

$$H_u = \frac{R + H_s}{\cos h_z} - R$$

where R is the radius of the earth.

15. The mean values of (H_s) and (H_u) found from the present Oslo observations are:

$$H_s = 43.7 \text{ km.} \quad H_u = 105.4 \text{ km.}$$

The observations from Oslo and Tromsø previously dealt with in the paper by Vegard and Tønsberg gave the somewhat greater mean values:

$$H_s = 54 \text{ km.} \quad H_u = 114 \text{ km.}$$

16. According to Vegard and Tønsberg the absorption of the effective ultra-violet radiation in the lower part of the atmosphere is caused by ozone, and the screening height found from the present observations is in good agreement with this hypothesis. In all cases the screening height is much greater than the height of maximum ozone concentration.

With respect to ultra-violet light there is a kind of "uviol twilight", determined by the "ozone shadow" with reference to the ultra-violet region of the solar spectrum.

17. The upper limit found for the D-emission in twilight and the appearance of the D-line in the auroral spectrum show that sodium is present in the highest strata of the atmosphere.
18. The intensity of the D-line is subject to great variations both in twilight and in the auroral luminescence. These fluctuations give further support to Vegard's hypothesis that sodium atoms or ions from the sun pass into the atmosphere.
19. The fact that the D-emission in twilight and in the auroral luminescence originates from the very highest strata of the atmosphere and the great intensity fluctuations show that Bernard's assumption of a terrestrial origin of the sodium engaged in the D-emission does not hold good.

Weighty arguments are also given against the meteorite-hypothesis of Cabannes, Dufay, and Gauzit.

The Physical Institute of the University, Oslo.

LIST OF PAPERS

1. L. Vegard: Geof. Publ. Oslo, Vol. IX, No. 11, 1932.
2. L. Vegard: G. P. O. Vol. X, No. 4, 1933.
3. L. Vegard: Phil. Mag. 46, 193 and 577, 1923. Zeitschr. f. Phys. 14, 376, 1923.
4. L. Vegard: Nordlicht, Handb. d. Exp. Phys. B. XXV, p. 453, 1928.
5. The Origin of the Red Colour of the Aurora etc. Det Norske Vid.-Akad., Avh. I, No. 2, 1926, Nature 117, 356, 1926.
6. L. Vegard and E. Tønsberg: Geof. Publ. V. XI, No. 16, 1937.
7. L. Vegard: Vorgänge und Zustände in der Nordlichtregion. Geof. Publ. XII, No. 5, 1938.
8. L. Vegard: Geof. Publ. XII, No. 14, 1940.
9. L. Vegard: Red and Sunlit Aurorae and the State of the Upper Atmosphere. Nature 138, p. 930, 1936.
10. L. Vegard: ZS. f. Phys. 106, p. 108, 1937.
11. L. Harang and W. Bauer: Gerlands Beiträge zur Geophys. 37, p. 109, 1932.
12. L. Vegard: Terr. Magn. 389, 1932.
13. L. Vegard and E. Tønsberg: G. P. XI, No. 2, 1935.
14. L. Vegard and E. Tønsberg: G. P. XII, No. 3, 1938.
15. L. Vegard: G. P. XII, No. 14, 1940.
16. L. Vegard and E. Tønsberg: G. P. XIII, No. 1, 1940.
17. L. Vegard and E. Tønsberg: G. P. XIII, No. 5, 1941.
18. L. Vegard and E. Tønsberg: G. P. XVI, No. 2, 1944.
19. L. Vegard: Enhancement of the Red Lines and Bands in the Auroral Spectrum from a Sunlit Atmosphere. Nature 137, p. 778, 1936.
20. L. Vegard and E. Tønsberg: ZS. f. Phys. 94, 413, 1935.
21. M. Nicolet: Naturwiss. 26, 839, 1938.
22. V. M. Slipher: Pub. A S. P. 41, 263, 1929.
23. J. Dufay: C. R. 194, 1897, 1932.
24. L. A. Sommer: ZS. f. Phys. 77, 374, 1935.
25. René Bernard: Nature 141, p. 788, 1938.
26. René Bernard: C. R. 206, p. 448, 1938.
27. René Bernard: C. R. 206, p. 928, 1137, 1669, 1938.
28. Georges Déjardin and René Bernard: C. R. 207, p. 81, 1938.
29. René Bernard: Astrophys. J. 89, 133, 1939.
30. Jean Cabannes, Jean Dufay, and Junior Gauzit: C. R. 206, 1525, 1938. Nature 141, 1054, 1938. Astrophys. J. V. 88, 164, 1938.
31. Garrigue: C. R. 205, 941, 1937.
32. L. Vegard: Coronal Phenomena and their Relation to Solar and Terrestrial Processes. G. P. Oslo Vol. XVI, No. 1, 1944.
33. R. Pendorf: Meteorolog. Z. S. 60, 401, 1943.
34. L. Vegard, Nature Vol. 145, p. 623, 1940.

PLATES

EXPLANATION OF PL. I

No. of Spectr.	Spectro-graph	Sort of Plate	Date	Interval of Exposure	Height	Direction	Remarks on Auroral Type
1	C	Agfa I.S.S.	$^{18}/_{9}$ 1941	21^{30}—23^{35}	ca. 20°	N	Various types
2	»	»	» »	23^{35}—01^{30}	ca. 45°	N	» »
3	»	»	$^{19}/_{9}$ »	01^{30}—03^{15}	low	N	R. and bright surfaces
4	»	»	» »	03^{15}—04^{15}	near Z		Corona
5	»	»	» »	04^{15}—04^{35}	»		Corona (violet R)
6	»	»	» »	20^{47}—21^{48}	10—20°	N	Lower part of A
7	»	»	$^{21}/_{9}$ »	22^{50}—04^{10}		N	Variety of types
8	»	»	$^{11}/_{10}$ »	21^{20}—00^{45}		N	» » »
9	»	»	$^{22}/_{10}$ »	18^{27}—18^{53}	6—10°	WNW	Sunlit A
10	»	»	» »	18^{53}—20^{55}	38—40°	N	Top of R
11	»	»	» »	20^{55}—22^{05}	13°	N—NE	Bottom R & D
12	»	»	» »	22^{05}—00^{06}	32°	N—NE	Top of R
13	»	»	$^{26}/_{10}$ »	21^{45}—22^{50}	8°	N	Various types
14	a	»	$^{5}/_{3}$ 1942	20^{20}—22^{40}	45°	N	Top of R
15	»	»	» »	22^{40}—00^{45}	11—12°	N	Lower edge of diff. A
16a	C	A.S.B.U.R.	» »	20^{15}—22^{10}	14°	N	Lower part of A
16b	»	»	» »	22^{10}—00^{45}	32°	N	Top of R and A
17	»	»	$^{19}/_{3}$ »	01^{00}—02^{50}	13°	N	Lower part of A
18	a	Agfa I.S.S.	$^{11}/_{9}$ »	20^{55}—21^{45}	15°	N	Lower part of A
19	»	»	» »	21^{45}—00^{25}	24°	N	Upper limit of A
20	»	»	$^{12}/_{9}$ »	00^{25}—01^{40}	28°	N	Top of R
21	»	»	» »	01^{40}—03^{15}	10°	N	Lower limit of R
22	C	Agfa I.S.S.	$^{11}/_{10}$ »	22^{00}—05^{00}	10°	N—N—W	Lower part of A
23	a	sens. NH_3	$^{8}/_{12}$ »	21^{15}—23^{30}	27°	N	Upper limit of A
24	»	»	» »	23^{30}—03^{30}	6.5°	N	Lower part of A
25	C	»	» »	21^{25}—23^{30}	16°	N	Upper » » »
26	»	»	» »	23^{30}—03^{30}	8°	N	Lower » » »
27	»	»	$^{11}/_{3}$ 1943	19^{52}—21^{07}	14°	N	Upper » » »
28	»	»	» »	21^{07}—01^{00}	7.5°	N	Lower » » »
29	»	»	$^{12}/_{3}$ »	01^{00}—04^{00}	15.5°	N	Upper » » »
30	»	»	» »	20^{20}—23^{50}	15.5°	N	» » » »
31	»	»	» »	23^{50}—03^{15}	10°	N	Lower » » »
32	»	»	$^{11}/_{4}$ »	22^{30}—00^{40}	6.5°	N	» » » »
33	»	»	$^{12}/_{4}$ »	00^{40}—01^{40}	19°	N	Upper » » »
34	a	»	$^{7}/_{10}$ »	19^{40}—22^{40}	12°	N	» » » »
35	»	»	» »	22^{40}—00^{45}	6°	N	Lower » » »
36	»	»	$^{8}/_{10}$ »	00^{45}—05^{15}	19°	N	Upper » » »

L means Lower Limit
U » Upper »
V » Strongest part of various forms
C » Corona, near point of convergence
S » Sunlit Aurorae.

a: $\lambda = 5577.35$ = Strong green OI-Line
b: $\lambda = 6300.3$ = » red OI-line

c: $\lambda = 6564$ = Hα
d: λ = so-called second "green line" composed of several lines and bands in the interval 5202—5250.
e: $\lambda = 5006.8$ = Nebular OIII-line.
f: $\lambda = 4861.5$ = Hβ.
g: $\lambda = 4709$ = Neg. Nitrogen band (0—2).
h: $\lambda = 4278$ = » » » (0—1).
i: $\lambda = 3914$ = » » » (0—0).

Pl. II No. 1: Enlarged Copy of No. 16 a of Pl. I
» » No. 2: » » » No. 16 b » » »

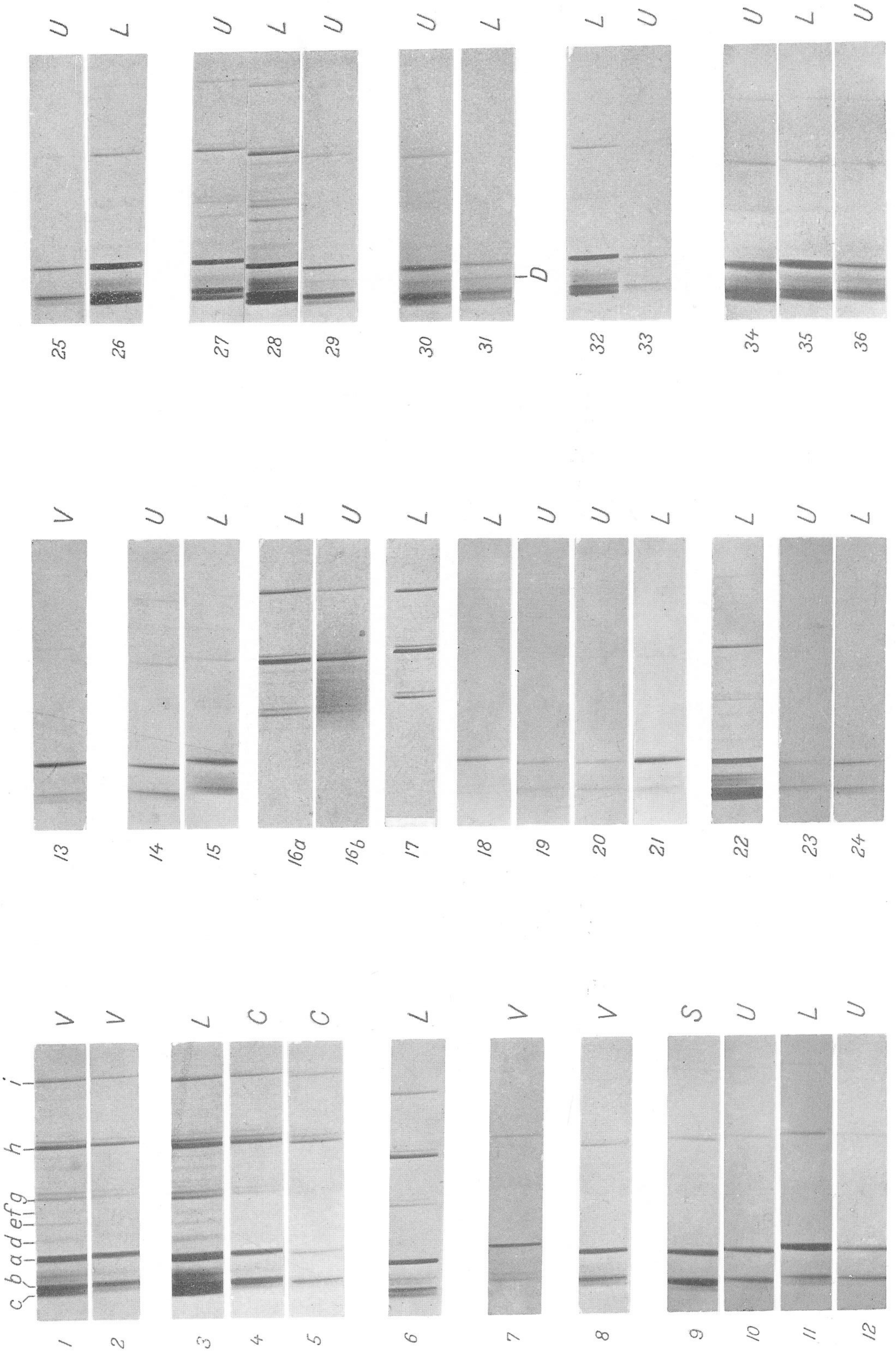
U
L
U
L
U
U
L
L
U
U
L
U
D
25
26
27
28
29
30
31
32
33
34
35
36
V
U
L
L
U
L
L
U
U
L
L
U
L
13
14
15
16a
16b
17
18
19
20
21
22
23
24
V
V
L
C
C
L
V
V
S
U
L
U
i
h
g
f
e
d
a
b
c
1
2
3
4
5
6
7
8
9
10
11
12

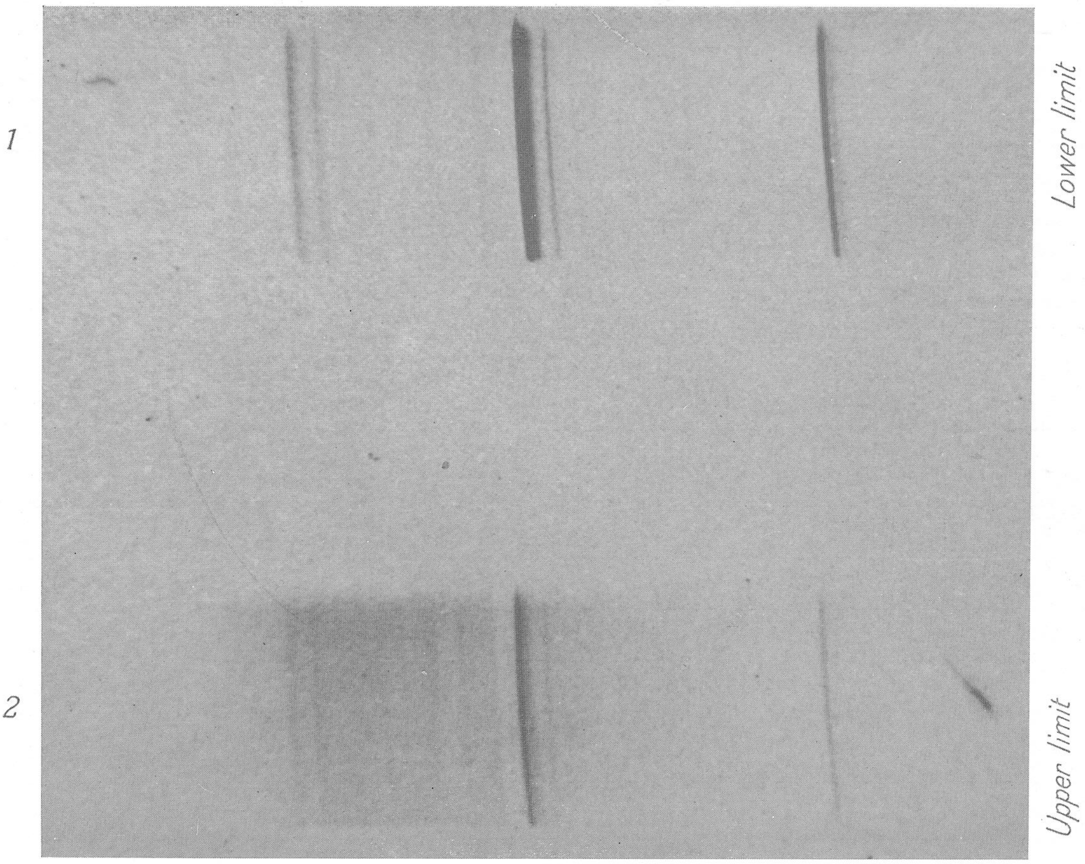
1
Lower limit
2
Upper limit

EXPLANATION OF PL. III.

Date	Nov. 30, 1942								
Remarks	Zenith, clear sky				h = 10°, clear sky				
Spectrum	a	b	c	d	e	f	g	h	i
Exposure	16^{15-18}	16^{18-23}	16^{23-32}	16^{32-44}	16^{47-50}	16^{50-56}	$16^{56}-17^{06}$	17^{06-20}	17^{20-45}

Date	Dec. 2, 1942						
Remarks	Zenith, hazy				h = 10°, haze below 9°		
Spectrum	a	b	c	d	e	f	g
Exposure	16^{13-16}	16^{16-21}	16^{21-30}	16^{30-42}	16^{50-54}	$16^{54}-17^{02}$	17^{02-16}

Date	March 19, 1943								
Remarks	Zenith, clear sky				h = 10°, clear sky				
Spectrum	a	b	c	d	e	f	g	h	i
Exposure	19^{07-09}	19^{09-14}	19^{14-25}	19^{25-36}	19^{38-42}	19^{42-48}	19^{48-57}	$19^{57}-20^{12}$	20^{12-27}

Date	March 23, 1943								
Remarks	Zenith, clear sky				h = 10, clouds lower down				
Spectrum	a	b	c	d	e	f	g	h	i
Exposure	19^{18-20}	19^{20-25}	19^{25-36}	19^{36-47}	19^{49-53}	19^{53-59}	$19^{59}-20^{08}$	20^{08-23}	20^{23-39}

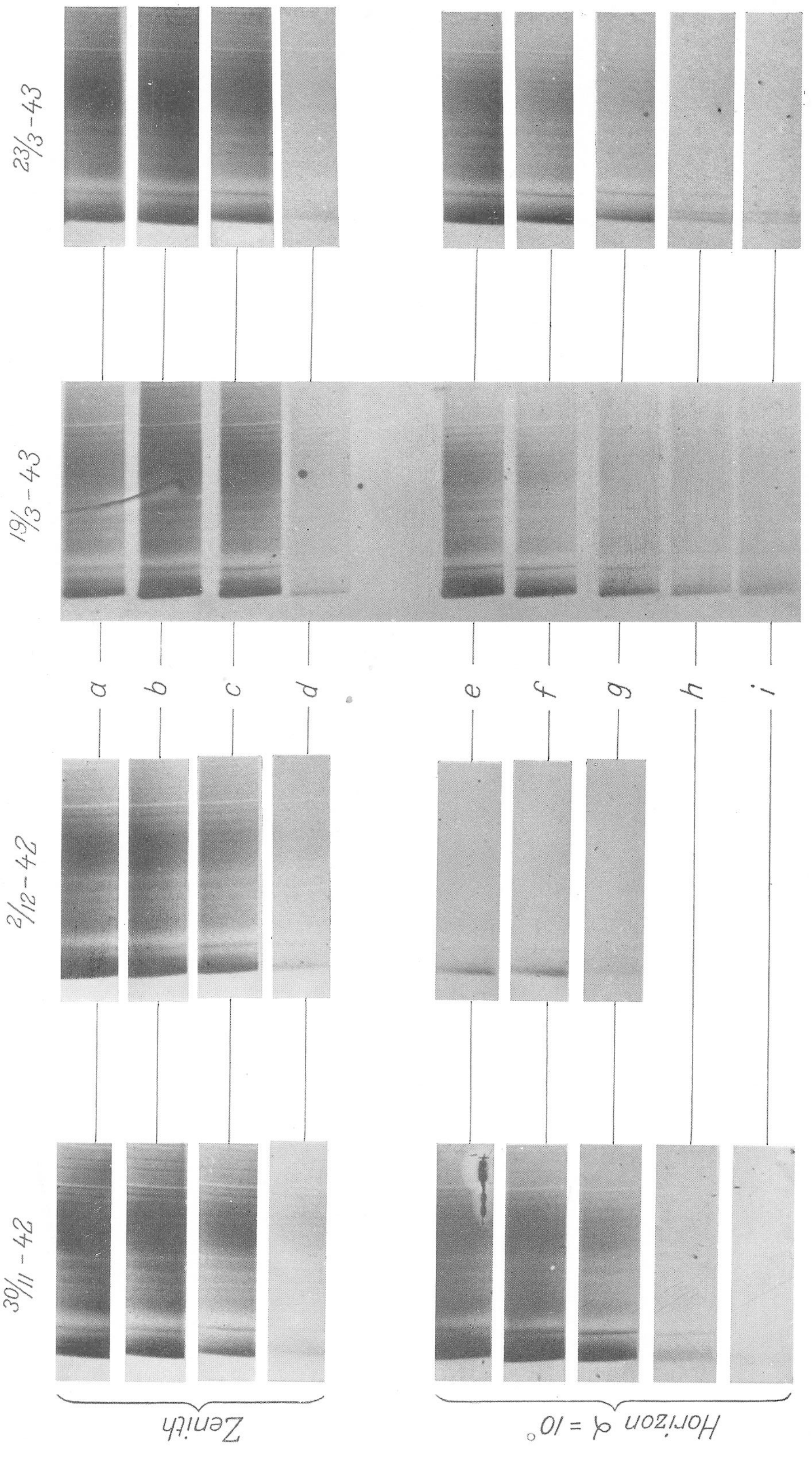
23/3-43
19/3-43
2/12-42
30/11-42
a
b
c
d
e
f
g
h
i
Zenith
Horizon α = 10°